# CHARACTERIZATION OF NEOGENE MARLS FROM THE KERT BASIN (N.E. MOROCCO): SUITABILITY FOR THE CERAMIC INDUSTRY

H. NASRI [A,*], A. AZDIMOUSA [A], K. EL HAMMOUTI [A], A. EL HADDAR [A], M. EL OUAHABI [B]

[A] *Laboratoire des Géosciences Appliquées, Faculté des Sciences, Université Mohammed Premier, Oujda, Morocco*

[B] *UR Argile, Géochimie et Environnement Sédimentaires (AGEs), Département de Géologie, Université de Liège, Liège, Belgium*

**corresponding author: h.nasri@ump.ac.ma*



**ABSTRACT:** The North-Eastern region of Morocco is filled with marine marls of Neogene age. The Neogene marls from the lower-Kert area were characterized to evaluate their suitability in the ceramic industry. To meet this objective, two cross-sections involving all the Neogene facies were performed

Mineralogical Society

This is a 'preproof' accepted article for Clay Minerals. This version may be subject to change during the production process.

DOI: 10.1180/clm.2019.50

on the both banks of the Kert River. Grey and green marls occurring between sandstone and tuffs were characterized by mineralogical (XRD) and physico-chemical analyses (grain-size, Atterberg limits, XRF, and specific surface area). The studied Neogene clays are mainly calcareous silty marls with $CaCO_3$ content ranging from 13 to 20 wt.%. The mineralogical composition showed the occurrence of quartz, calcite, feldspars, dolomite, illite, kaolinite, chlorite, and mixed-layers (10-14 Å). Cristobalite occurred only in the uppermost level of the green marls supplied from volcanic ash during the Messinian. Siderite and rhodochrosite occurred as traces pointing out to reducing or locally oxidizing conditions during sedimentation or shortly thereafter. There, marls have medium to high plasticity that is optimum for extrusion. Raw Neogene marls are suitable for structural clay products manufacturing. More specific uses were supported by geochemical results and grain-size distribution as hollow products, roofing tiles, and masonry bricks.



**KEYWORDS:** ceramic, geochemistry, marl, Kert, Morocco, Neogene, Rif.

## INTRODUCTION

Large tonnages of clay materials are used in ceramic industry such as common bricks, structural bricks, refractories, pottery products, stonewares, sanitary wares, and roofing tiles (Murray, 1994; Harvey & Lagaly, 2006; Reeves *et al.*, 2006; Murray, 2007; Keith & Murray, 2009; Petrick *et al.*, 2011; Mukherjee, 2013). Mineralogical, chemical, and grain-size distributions of clays determine their engineering properties (Harvey & Lagaly, 2006; Keith & Murray, 2009). Due to their plastic behavior, clay materials could be worked in many desired shapes, dried, and fired to produce products with high hardness (Murray, 1994). Morocco is one of the most producers and consumers of clayey building materials. In particular, the Rif area (Northern Morocco) is mostly filled with clays of Neogene age (El Ouahabi, 2013; Mesrar *et al.*, 2013; El Ouahabi *et al.*, 2014a; El Ouahabi *et al.*, 2014b). These clayey materials have particularly drawn attention since few years ago.

In the Northwest of Morocco (Tetouan area), sandy marls of Late Pliocene age showed high content of illite/muscovite (43-57 %) and clay minerals (30 %). The clay fraction consists mostly of illite (88 %). These Pliocene clays are silty clay (92 % of 2-20 µm fraction), with low to medium plasticity and are suitable for structural clay products (El Ouahabi *et al.*, 2014a; El Ouahabi *et al.*, 2014b).

In the Tangier region (N.W. Morocco), Pliocene marls are sandy clay with variable mineralogical composition. The total clay minerals and quartz content are 24-48 % and 29-61 %, respectively. The clay fraction is dominated by illite (56-82 %). These marls are silty clay (70-88 % of 2-20 µm fraction) and have medium plasticity. These materials are suitable for clay roofing tiles and structural clay products (El Ouahabi *et al.*, 2014b).

In the Center-North Morocco (Meknes region), Miocene yellow sandy marls from the Saïs Basin are mostly homogeneous. They consist of total clay (27-45 %), quartz (19-27 %), and calcite (20-28 %). Illite (45-58 %) always dominates with the occurrence of variable amount of smectite. These marls are therefore illitic, very plastic, and suitable for structural clay products (El Ouahabi *et al.*, 2014a; El Ouahabi *et al.*, 2014b). In Fez region (Center-North Morocco), Miocene gray marls are also illitic clays (37-46 % of illite), having medium to high plasticity. They are illitic silty clay, containing 23-37 % of total clay. As Miocene marls from the Meknes area, the Fes raw marls are suitable for structural clay products (Mesrar *et al.*, 2013). Furthermore, similar composition is found in Miocene marls from the Taza region (Center-North Morocco) displaying the presence of quartz, calcite, dolomite, illite, and kaolinite (Mesrar *et al.*, 2017).

The Neogene deposits from North-East of Morocco have been the subject of geological, sedimentological, paleontological, and structural studies (Guillemin & Houzay, 1982; Frizon de Lamotte & Leikine, 1985; Essafi, 1986; Asebriy *et al.*, 1993; Azdimousa & Bourgois, 1993; Abdellah, 1997; Cunningham *et al.*, 1997; El Bakkali *et al.*, 1998a; El Bakkali *et al.*, 1998b; Cunningham & Collins, 2002; Azdimousa *et al.*, 2006; Münch *et al.*, 2006; van Assen *et al.*, 2006; Chalouan *et al.*, 2008; Achalhi, 2016; Achalhi *et al.*, 2016; Cornée *et al.*, 2016; Nasri *et al.*, 2016). However, there are no previous studies dealing with Neogene marls in the area because of the inaccessibility of this mountainous region, particularly with the lack of infrastructure. This problem has recently been resolved thanks to the construction of the coastal road connecting the east (Saïdia) to the west (Tangier) regions of Morocco. Within this context, the current study aims to characterize the clayey materials from the lower part of the Kert Basin (North-Eastern Rif) and to evaluate their suitability for ceramic production through mineralogical, geochemical, and geotechnical properties. (Dondi *et al.*, 2014) proposed an industry-oriented technological classification of clay raw materials, on the basis of chemical ($Fe_2O_3$ content), clays and carbonates mineralogy, particle size and plasticity. The potentiality of Neogene marls for ceramic applications will be evaluated based on characterization

study. For this purpose, two geological cross-sections were performed on the both banks of the Kert River.

## GEOLOGICAL SETTING

The geological history of the Rif area began since Late Cretaceous at the time of closure of Tethys oceanic domain (Michard *et al.*, 2002). Since, two periods of relatively rapid convergence during Late Cretaceous and Eocene-Oligocene occurred, alternated with periods of slower convergence during Paleocene and since Early Miocene (Rosenbaum *et al.*, 2002). Since Middle Miocene, an E-W extension have lead the individualization of Neogene post-nappes basins in the Rif area during Tortonian, including the Kert Basin (Guillemin & Houzay, 1982; Achalhi, 2016; Achalhi *et al.*, 2016). Since Late Tortonian, a strong convergence associated with intense volcanism in the eastern Rif area has led Africa to move in the N.W. direction (Guillemin & Houzay, 1982; Mazzoli & Helman, 1994). Consequently, the Kert Basin, as other Neogene basins of the region, was exposed to abundant marly sedimentation during Miocene.

Due to its large surface area, the Kert Basin is divided into two parts (Guillemin & Houzay, 1982): (1) Lower-Kert is located in the western part of the Melilla-Nador Basin and continues to the Beni Saïd mountain. (2) Upper-Kert extends from the Beni Bou Ifour massif in the East, to the Tizi Ouzbar schist (west of

Midar city) in the west. This latter is limited to the north-west by the Bou Ziza volcano and to the north-east by the Gourougou volcano (FIG. 1).

The Neogene of the Kert Basin is characterized by a basal conglomerate located on westward of the Beni Saïd (Guillemin & Houzay, 1982; Essafi, 1986) and Zeghanghane Mountains suggesting a deepening due to the occurrence of syn-sedimentary faults affecting the thickness of the series towards the west of the basin (Essafi, 1986; Abdellah, 1997). Marl associated with interstratified levels of rhyolitic tuffs-cinerites layers were deposited above the conglomerate in a deep Messinian sea (Essafi, 1986). In the lower-Kert area, the post-nappes series are Messinian with a clearly transgressive behavior submerging the Beni Saïd Mountain (eastern Temsamane), setting up a marly sedimentation started with detrital conglomerate and sandstone, overcoming the Beni Saïd Mountain in the West of the basin. Then, the facies becomes marly, with cinerite intercalations due to the Messinian volcanic activity, from the bottom of the mountain to the S.W. of the Melilla Basin (Guillemin & Houzay, 1982). Interbedded pyroclastic levels (tuffs and cinerites) in the Messinian marls could be used for stratigraphic correlations because of their large extension (Abdellah, 1997). More recent $^{40}Ar$ / $^{39}Ar$ dating works have assigned a date of 6.9 ± 0.02 Ma at the basal level of the Izaroren cross-section (Cunningham *et al.*, 1997; van Assen *et al.*, 2006). The end of open marine deposits was carried out before

6 Ma (van Assen *et al.*, 2006) confirming the Messinian age of marls from the Lower-Kert area. Like the neighboring sedimentary basins, the Late-Messinian regression is recorded in the Kert Basin (Guillemin & Houzay, 1982).

## MATERIALS AND METHODS

### *Materials*

Sampling was carried out in the Messinian marly sediments of the Lower-Kert area, along two cross-sections; Izaroren and Afza located on either sides of the Wadi Kert mouth (FIG. 1). The thickness of each section exceeds 100 meters. A total of five marly samples, labeled Izar 1, Izar 3, Izar 4, Izar 5, and Izar 6, were sampled from the Izaroren profile (east of the Wadi Kert) (FIG. 2). A total of four samples were also taken from the Afza cross-section (west of the Wadi Kert), labeled Af 1, Af 3, Af 4, and Af 5 (FIG. 3). The sampling locations have been chosen in marly facies away from trees, shrubs, and anthropogenic influences. The sampling has been performed by digging deep into the formation after removing the altered surface, and then sampling a fairly sufficient amount of material. In addition to correlate the two profiles, three more samples have been taken from tuff levels: Izar 2 from Izaroren cross-section; Af 2 and Af 6 from Afza cross-section.

*Experimental methods*

The studied samples were subjected to mineralogical and geochemical analyzes to estimate bulk and clay mineralogical composition, and determine the main major chemical elements. The calcimetry and grain-size analyzes allowed to determine the $CaCO_3$ content, and the < 2 µm, 2-20 µm, and > 20 µm fractions, and the sedimentological fractions (< 4 µm; 4 µm-63 µm; 63 µm-2 mm) according to Wentworth scale (Wentworth, 1922). The Atterberg limits and methylene blue values allow the determination of the marls plasticity level, their extrudability, and their specific surface area.

*Mineralogical and chemical analysis*

To characterize the Messinian marls and tuffs belonging to the both studied profiles, mineralogical and geochemical analyzes were performed. The bulk samples were prepared by grinding about 1 g of dried sample in a mortar, and then placed into a sample holder in order to limit any preferential orientation of minerals (Moore & Reynold, 1997; Boski *et al.*, 1998; Fagel *et al.*, 2003).

The mineralogical composition (XRD) was carried out using an XPERT-PRO diffractometer with Cu-Kα radiation (λ = 1.5418 Å), at the National Center for Scientific and Technical Research - Technical Support Unit for Scientific Research (UATRS-CNRST), Rabat, Morocco. The X-ray patterns were

analyzed using X'Pert HighScore Plus software and PDF-2 database. Semi-quantitative estimation of mineralogical phases was obtained by multiplying the measured intensity of specific reflection by corrective factors to obtain the amount of each mineral (Cook *et al.*, 1975; Boski *et al.*, 1998; Fagel *et al.*, 2003).

Oriented aggregates using the Glass Slide Method (Moore & Reynold, 1997) on the < 2 μm fraction were only performed on marly samples. The clay fraction was obtained by suspension in distilled water of about 1 g of dried bulk sediment, previously sieved at 63 μm. The samples were decarbonated with HCl (0.l mol/L) and thereafter washed enough with distilled water, and the supernatant was removed by centrifugation. The < 2 μm fraction was separated after a settling time by gravity sedimentation following Stoke's law (AFNOR, 1992; Moore & Reynold, 1997). The first centimeter of the suspension was placed on a glass slide and dried overnight at room temperature. The XRD clay analyzes included the successive measurement of an X-ray patterns in air-dried (AD), after solvation with ethylene glycol for 24 h (EG), and after heating at 500°C for 4 h (500°C) (Moore & Reynold, 1997). This last treatment allows to characterize some hydrated minerals and to distinguish between the contribution of kaolinite and chlorite at ~7.1Å. The (001) peak of kaolinite disappears after heating at 500°C, while the (002) peak of chlorite persists at

~7.0Å (Moore & Reynold, 1997; Fagel *et al.*, 2003; Fagel & Boës, 2008). Semi-quantitative estimations of the main clay phases were obtained from the measured intensity of a diagnostic peak multiplied by the corrective factors (Biscaye, 1965; Cook *et al.*, 1975; Fagel *et al.*, 2003; Fagel *et al.*, 2007; Nkalih Mefire *et al.*, 2018) (FIG. 4 and 5).

The chemical analysis of the major elements has been performed on Axios X-Ray Fluorescence spectrometer with wavelength dispersion (1 kW), at the National Center for Scientific and Technical Research - Technical Support Unit for Scientific Research (UATRS-CNRST, Rabat, Morocco). The results have been expressed in mass percentage of oxides. The Loss On Ignition (L.O.I) was obtained by heating the samples at 1000°C during 2 h under oxidizing conditions.

The $CaCO_3$ content has been measured using a Bernard calcimeter; based on the volume of carbon dioxide ($CO_2$), according to the French Standard NF P 94-048 (AFNOR, 1996).



*Physical and textural analyzes*

Particle-size distribution has been obtained by wet sieving through an 80 µm sieve. The < 80 µm particles was then suspended in water mixed with a dispersant (sodium hexametaphosphate: $Na_6$ $(PO_3)_6$, $10H_2O$), and shacked in

order to avoid any agglomeration of clay particles, according to the French Standard NF P 94-057 (AFNOR, 1992). The evolution over time of the solution density was measured by an apparatus called a hydrometer. The maximum diameter and the mass percentage of sedimented particles are calculated based on the measured densities.

The Atterberg limits, including liquid limit (LL), plastic limit (PL), and plasticity index (PI) were determined by the Casagrande method according to the French Standard NF P 94-051 (AFNOR, 1993). The methylene blue amount absorbed by the clay sample allowed to determine the capacity of clay to adsorb cations from a solution, and thereby predicts how the clay will react, based on cation-exchange capacity (CEC). Clay minerals are negatively charged owing to the presence of permanent charges due to isomorphous substitutions in the octahedral and tetrahedral sheets and the formation of negative charges at the edges (Ammann *et al.*, 2018). The CEC is the capacity of clay to hold cations in order to balance this negative charge. The Specific Surface Area (SSA) has been calculated using the methylene blue index method according to the French Standard NF P 94-068 (AFNOR, 1998). The SSA was calculated by the following equation (AFNOR, 1998):

$$SSA = MBV\ (C_{MB}*N_{av}*A_{MB}/1000\ M_{MB})$$

$$MBV = V_{MB}*C_{MB}*100/w_0$$

Where $C_{MB}$ is the concentration of methylene blue solution (10 g/L), $N_{av}$ is the Avogadro number (6.02 $10^{23}$), $A_{MB}$ is the area covered by one methylene blue molecule (130 $Å^2$), $M_{MB}$ is the molar mass of methylene blue (319.85 g/Mol), MBV is the methylene blue value (g/100g of sample), $V_{MB}$ is the volume of methylene blue solution injected to the soil solution (ml), and $w_0$ is the dry weight of the sample used (g).

## RESULTS

### *Lithological description*

In the lower part of the Kert Basin, two cross-sections located on both banks of the Kert River were investigated; the Izaroren cross-section to the east and the Afza cross-section to the west. The maximum depth of both profiles not exceeds 100 m (FIG. 2 and 3).

The Izaroren profile begins with gray marl outcropping over about 10 m-thick. This marl is devoid of visible fossils. It is surmounted by a whitish tuff layer of 8 m-thick, rich in quartz and feldspars, and is rhyolitic in nature (El Bakkali *et al.*, 1998a). The series continues with a thick grayish marl layer of about 80 m-thick without visible macrofossils, which becomes gypsiferous at the top (FIG. 2). The profile ends with a succession of 6.5 m-thick indurated sandstone marl

and greenish marly layers of 20-15 m-thick with some ferruginous features, probably reflecting the beginning of the Late-Messinian regression.

The Afza profile is remarkably affected by normal faults attesting for the Messinian syn-sedimentary subsidence (FIG. 3). At the base, as the Izaroren profile, a greenish marly layer of 10 m-thick with some yellowish patches occur. It is topped by a whitish tuff layer of 2 m-thick. In the Afza profile, succession of at least two gray marly layers (12-15 m) alternates with two conglomeratic banks of sandy breccias (5-7 m) and affected by normal faults. These marls are gray with red ferruginous features. This alternation is surmounted by a sandbar of about 4 m-thick, showing bioturbations and ferruginous features on its upper surface. The series continues with green plastic marly sediment of 45 m-thick, topped by a slightly altered white volcanic tuff of about 12 m-thick.



*Marl characteristics*

The mineralogical composition (TABLE 1) mostly showed quartz (12-25 wt.%), total clay (38-58 wt.%), and calcite (13-32 wt.%), associated with minor amounts of feldspars (3-15 wt.%) and dolomite (1-5 wt.%). While siderite (0-1 wt.%) and rhodochrosite (0-2 wt.%) occur in traces. Cristobalite occurred only in Izar 6 (22 wt.%) and Af 5 (6 wt.%). The amount of quartz was slightly

smaller in Izaroren marly samples (12-18 wt.%) than in Afza (22-25 wt.%). Conversely, total clay amount was greater in the Izaroren (39-58 wt.%) than in the Afza profile (38-46 wt.%). The clay fraction (< 2 µm) significantly vary; it consisted of illite (28-46 wt.%), kaolinite (2-27 wt.%), and mixed-layers 10-14 Å (26-48 wt.%). Chlorite occurred from 11 wt.% to 29 wt.%, but was absent in the uppermost samples of the Izaroren and Afza profiles (in samples Izar 6 and Af 5).

The chemical composition of studied marly samples (TABLE 2) showed that the main oxides are $SiO_2$ (38.3-54.8 wt.%), $Al_2O_3$ (8.5-13.1 wt.%), $Fe_2O_3$ (9.1-16.6 wt.%), and CaO (6.6-9.2 wt.%). Whereas, $TiO_2$ (0.37-0.65 wt.%), MgO (1.75-2.98 wt.%), $K_2O$ (1.09-1.67 wt.%), $Na_2O$ (1.04-4.28 wt.%), $SO_3$ (0.3-1.1 wt.%), $MnO_2$ (0.29-0.51 wt.%), and $P_2O_5$ (0.15-0.2 wt.%) were present in small amounts. The L.O.I values varied between 11.37 wt.% and 16.85 wt.% due mainly to the variable amount of carbonates and clay minerals. The amount of carbonate (TABLE 3) was varying between 13 wt.% and 20.4 wt.%, which is characteristic of marly facies.

The TGA-DTA curves of the Izaroren 4 marl is shown in FIG. 6. The DTA curves display four endothermic and two exothermic peaks. The first endothermic peak is situated at ~100 associated with loss on weight of 3.6 wt.% due to the removal of physisorbed water. An exothermic peak appears at ~160

°C which is attributed to the burning of organic matter. The second endothermic peak is situated at about 550°C and associated with relatively high weight loss of 5.86 wt.%, assigned to dehydroxylation of kaolinite into metakaolinite (Brindley and Nakahira, 1959; Shvarzman *et al.*, 2003). The third and fourth endothermic peaks at ~730 and ~850°C are associated with slightly high loss on weigh of 5.1 wt.% due to decomposition of calcite and dolomite respectively (Alvares *et al.*, 2000). A small exothermic peak at ~900°C associated with small loss on weight of 0.6 wt.% is related to crystallization of intermediate Ca-silicates phases and most likely the inception of aluminosilicates (spinel) formation (Trindade *et al*., 2009; El Ouahabi *et al*., 2015; Milošević & Logar, 2017).

The grain-size data showed significant variations along the profiles, implying lateral and vertical variation within the deposit (TABLE 3). Hence, along the Izarouren section, the grain-size fractions did not show a huge regularity (FIG. 7. A). Thus, sand (> 63 µm) content is 9 wt.% in the Izar 6 sample, but it didn't exceed 3 wt.% in the other samples of the Izaroren profile. Nevertheless, silts (4-63 µm) showed variable amounts (26-75 wt.%) over the depth. The < 4 µm fraction varies from 23 to 71 wt.%, which inversely varies with the silt (4-63 µm) amount.

In the Afza section, more regular variations in clay, silt, and sand fractions were observed (FIG. 7. B). Thus, the sand content increased gradually from the base of Afza profile (10 wt.%) to the top (18 wt.%). Similarly, the silt content increased from 28 wt.% at the base to 49 wt.% at the top, and from 29 wt.% to 37 wt.% in the middle part of the profile. However, the clay content gradually decreased from the bottom (60 wt.%) to the top (32 wt.%).

The differences in mineralogical and grain-size properties are also shown on geotechnical data (TABLE 3). The liquid limit (LL), plastic limit (PL), and plasticity index (PI) varied from 44 % to 72 %, from 20 % to 45 %, and from 23 % to 45 %, respectively. The SSA values showed a huge variation, ranging from 26.3 $m^2/g$ to 125.6 $m^2/g$.

## DISCUSSION

### *Characterization of Miocene marls*

Mineralogical analysis allowed to correlate between the lithologies of the two cross-sections. Thus, the two profiles can be subdivided into two parts: (1) gray marl in the lower part, and (2) green marl in the upper part (FIG. 8). In addition, total clay amount inversely varied with the content of quartz and cristobalite. At the top of the two profiles, a slight decrease in total clay from 43 to 39 wt.% and from 42 to 38 wt.% occurred in the Izaroren and Afza profile, respectively.

This decrease is associated with the appearance of cristobalite (22 and 6 wt.% in uppermost samples of the Izaroren and Afza profiles respectively). Likewise, chlorite inversely varied with the abundance of illite and kaolinite, and definitively disappeared at the top of the two profiles (Table 1). The late appearance of cristobalite is due to the Messinian volcanism characterizing the eastern Rif, supported by the disappearance of chlorite and the establishment of the tuff overlying the green marl in the Afza profile.

These marls are rich in calcite, which is basically of biological marine origin (planktonic and benthic) and also could have a continental origin. Traces of siderite and rhodochrosite were formed in the sediments during their deposition or shortly thereafter. In fact, they point out to reducing or locally oxidizing conditions.

The chemical composition is in accordance with mineralogical composition. So, the high content of $SiO_2$ is mainly related to the high amount of clay minerals, quartz, and also the presence of cristobalite in samples Af 5 ($SiO_2$ = 46.37 wt.%) and Izar 6 ($SiO_2$ = 54.8 wt.%). The $Al_2O_3$ and CaO amounts are mostly associated respectively with total clay and calcite abundance. The L.O.I values vary between 11.4 wt.% and 16.8 wt.% which is related to the presence of clay minerals, hydroxides, organic matter, and carbonates (Milheiro *et al.*, 2005; Baccour *et al.*, 2008).

Along the Izaroren profile, the Shepard grain-size classification (Shepard, 1954) classified samples Izar 1 and Izar 4 in silty clay field. Whereas, the other samples (Izar 3, Izar 5, and Izar 6) were clayey silts (FIG. 9). This grain-size irregularity was mainly due to hydrodynamic fluctuations during sedimentation. According to the Shepard classification (Shepard, 1954), the uppermost sample (Af 5) of the Afza cross-section was clayey silt. The other samples were silty clays (FIG. 9). The progressive evolution of the different particle size fractions over depth was due to gradual increase in hydrodynamic energy during deposition.

The mineralogical composition of the Messinian marls form the Lower-Kert area displayed similarities with Neogene marls from the Sais Basin in Meknes area (Morocco) (El Ouahabi *et al.*, 2014b). However, the studied marls of the Lower-Kert area contained 10-14 Å mixed-layers clays instead of smectite in the Meknes marls. Furthermore, similar mineralogical composition has been observed for the Algerian Neogene clayey deposits from Jijel Basin (Baghdad *et al.*, 2017), but with a greater amount of kaolinite than the Lower-Kert marls. Both Neogene marls are successfully used for structural clay products (El Ouahabi *et al.*, 2014b; Baghdad *et al.*, 2017).

The variations in mineralogical and grain-size results mainly affected the geotechnical properties. The Atterberg limits showed that the samples Af 3 and

Af 4 were medium plastic, whereas the other studied samples were highly plastic (FIG. 10).

SSA depends on several parameters like the quantity and mineralogy of clay minerals, CEC, and grain-size of the materials (De Kimpe *et al.*, 1979; Tiller & Smith, 1990; Petersen *et al.*, 1996; De Jong, 1999). The SSA (26.3-125.6 $m^2/g$) values of the Lower Kert marls were considered low even though they are greater than the Meknes marls values (33.3-37.9 $m^2/g$). The Lower-Kert marls belonged to the SSA intervals of kaolinite (10-30 $m^2/g$), illite (70-140 $m^2/g$), and chlorite (50-150 $m^2/g$); and they were much lower than smectite (700-800 $m^2/g$) and vermiculite (760 $m^2/g$) ones (Beaulieu, 1979; Mahmoudi *et al.*, 2017), which was consistent with the mineralogical data.

*Ceramic suitability*

The suitability of raw clay deposits for ceramic applications is determined by their physical properties, mineralogy, and chemistry (El Ouahabi *et al.*, 2014b; Lisboa *et al.*, 2016; Baghdad *et al.*, 2017; Kharbish & Farhat, 2017; El Boudour El Idrissi *et al.*, 2018). The bulk mineralogical association of studied samples and the dominance of illite in their clay fractions classified these marls as common clays (Murray, 2007; Keith & Murray, 2009), and gave them suitable ceramic properties (Ferrari & Gualtieri, 2006; Wattanasiriwech *et al.*, 2009;

Baghdad *et al.*, 2017; Mahmoudi *et al.*, 2017). According to the Strazzera ternary diagram (Strazzera *et al.*, 1997) (FIG. 11), the top sample of the Afza profile (Af 5) was suitable for clay roofing tiles. The other samples were within the field of structural clay products, except the bottom-most sample of the Izaroren profile (Izar 1). The samples Af 5, Izar 1, and Izar 6 were extremely plastic. They require some processing such as the addition of coarse materials (*e.g.* quartz, feldspar, and chamotte) to decrease the plastic behavior of their higher clay content. The other samples were medium to highly plastic marls suitable for extrusion (Fig. 12).

According to Winkler (Winkler, 1954) and based on grain-size results (FIG. 13), Af 1 and Izar 4 samples belonged to roofing tiles and masonry bricks field. While, the samples Af 3, Af 4, Af 5, and Izar 1 were suitable for hollow products. Nonetheless, the sample Izar 1 requires some pretreatments to make it suitable because of its relatively high content of clay fraction. In comparison, Neogene marls from Jijel Basin (Algeria) are situated between the hollow products and roofing tiles-masonry bricks fields (Baghdad *et al.*, 2017), while marls from Meknes (Morocco) are out of domains of suitability, because of their high silt content (El Ouahabi *et al.*, 2014b).

According to the $(Al_2O_3)$-$(Fe_2O_3+CaO+MgO)$-$(Na_2O+K_2O)$ ternary diagram (FIG. 14) (Fiori *et al.*, 1989), all Afza samples, and samples Izar 3 and Izar 4

from the Izaroren marls belonged to red ceramic field. The studied marls were moderately rich in CaO acting as fluxing agents (Trindade *et al.*, 2009; Trindade *et al.*, 2010), which allows to predict the transformation of high-temperature minerals in ceramic products (Trindade *et al.*, 2010; EL Ouahabi *et al.*, 2016). The higher amount of $Fe_2O_3$ (> 5 wt.%) could give all samples a reddish color after firing (Abajo, 2000; Ngun *et al.*, 2011), and made them inappropriate for fine ceramics without any processing to dilute the iron oxide content. Comparable $Fe_2O_3$ amounts were also detected in the Neogene marls from Meknes (12.16 - 16.63 wt.%) making them unsuitable for fine ceramics (El Ouahabi *et al.*, 2014a). Much lower amounts were found in the Neogene marls from Jijel Basin (Algeria) deposits (4.89 - 8.08 wt.%) (Baghdad *et al.*, 2017). Similar iron oxide percentages (4.21-8.61 wt.%) with high carbonate content (20-25 wt.%) were showed on the Tertiary marls from the Bailén area in southern Spain. These marls are suitable for making porous red wall tiles, clinker, vitrified red floor tiles and porous light-coloured wall tiles by pressing (Gonzalez *et al.*, 1998).

In the north-western Mediterranean, Tertiary marls from Castellon area (Spain) have much lower iron oxide percentages (3.75-6.10 wt.%) with wide and variable amount of CaCO3 (16-27 wt.%) (Jordán *et al.*, 2001). Likewise, Plio-Pleistocene marls from the Sassuolo District (Italy) show low iron oxide

amount (4.5-6 wt.%), with large variability in carbonate content (15-25 wt.%) and MgO (Dondi, 1999).

Due to the occurrence of sulfate and sodium associated of high amount of calcium in the most of marls studied (Table 2), efflorescence phenomenon can be produced during firing (González *et al*., 2006; Andres *et al*., 2009). This phenomenon can be controlled by monitoring the firing parameters such the rate of heating and the level of the firing temperature (Andres *et al*., 2009).



## CONCLUSIONS

Neogene clayey deposits located on the Kert River banks (North Eastern Rif, Morocco) were characterized and their suitability for ceramic manufacture was also discussed.

The mineralogical composition mainly consisted of quartz, calcite, and total clay fraction. The latter consisted of illite, kaolinite, mixed layers (10-14 Å), and chlorite. Such composition qualified these materials as common clays. The chemical composition of these marls was in agreement with mineralogical composition. The main oxides were $SiO_2$, $Al_2O_3$, $Fe_2O_3$, and CaO. Mineralogical and geochemical data confirmed the occurrence of the volcanism relicts recorded in the Messinian sedimentary series. The studied Neogene clay deposits were marly silts or silty marls with medium to high plastic behavior.

The marls of the Lower Kert were suitable as a potential raw material for ceramic industry. These raw marls could be used in the manufacturing of structural clay products, especially hollow products, roofing tiles, and masonry bricks excluding Izar 1 sample which requires processing to make it suitable for this ceramic kinds. Some marl samples were appropriate for optimal (Af 3, Af 4, and Izar 4) or acceptable (Af 1, Izar 3, and Izar 5) extrusion. The remaining samples (Af 5, Izar 1, and Izar 6) need additional treatments or formulations because of their high plasticity. Sand or chamotte addition is necessary to produce extruded ceramic.

**References**


Abajo, M. (2000). *Manual sobre fabricación de baldosas, tejas y ladrillos*. Beralmar S. A., Barcelona.

Abdellah, R. (1997). *Les bassins néogènes du sillon sud-rifain et du Rif nord oriental (Maroc): sédimentologie, paléontologie et évolution dynamique.* Docteur Es-Sciences. Sidi Mohammed Ben Abdellah, Fes, Maroc.

Achalhi, M. (2016). *Chronostratigraphie et sédimentologie des bassins néogènes de Boudinar et d'Arbaa Taourirt (Rif oriental, Maroc).* Docteur en sciences. Mohamed Premier, Oujda, Maroc.

Achalhi, M., Münch, P., Cornée, J.-J., Azdimousa, A., Melinte-Dobrinescu, M., Quillévéré, F., Drinia, H., Fauquette, S., Jiménez-Moreno, G., Merzeraud, G., Moussa, A.B., El Kharim, Y. & Feddi, N. (2016). The late Miocene Mediterranean-Atlantic connections through the north rifian corridor: New insights from the Boudinar and Arbaa Taourirt basins (northeastern Rif, Morocco). *Palaeogeography, Palaeoclimatology, Palaeoecology*, **459**, 131-152.

AFNOR. (1992). Norme française. Sol: Reconnaissance et essai. Analyse granulométrique des sols. Méthode par sédimentation. Pp. 17. *NF P 94-057*, AFNOR.

AFNOR. (1993). Norme française. Sols: Reconnaissance et essais. Détermination des limites d'Atterberg: Limite de liquidité à la coupelle-limite de plasticité au rouleau. Pp. 15. *NF P 94-051*, AFNOR.

AFNOR. (1996). Norme française. Sols: Reconnaissance et essais. Détermination de la teneur en carbonate. Méthode du calcimètre. Pp. 11. *NF P 94-048*, AFNOR.

AFNOR. (1998). Norme française. Sol: Reconnaissance et essais. Mesure de la capacité d'adsorption de bleu de méthylène d'un sol ou d'un matériau rocheux. Pp. 8. *NF P 94-068*, AFNOR.

Alvares, J. I., Navarro, I., and Garcia Casado, P. J. G. (2000). Thermal, mineralogical and chemical studies of the mortars used in the cathedral of Pamplona, Spain. *Thermochim Acta* **365**(1–2): 177–187.

Ammann, L., Bergaya, F. & Lagaly, G. (2018). Determination of the cation exchange capacity of clays with copper complexes revisited. *Clay Minerals*, **40**, 441-453.

Andres, A., Díaz, M. C., Coz, A., Abellán, M. J., & Viguri, J. R. (2009). Physico-chemical characterisation of bricks all through the manufacture process in relation to efflorescence salts. *Journal of the European Ceramic Society*, **29(10)**, 1869-1877.

Asebriy, L., Bourgois, J., Cherkaoui, T.E. & Azdimousa, A. (1993). Evolution tectonique récente de la zone de faille du Nékor : Importance paléogéographique et structurale dans le Rif externe, Maroc. *Journal of Africain Earth Sciences*, **17**, 65-74.

Azdimousa, A. & Bourgois, J. (1993). Les communications entre l'Atlantique et la Méditerranée par le couloir sud-rifain du Tortonien à l'Actuel: Stratigraphie séquentielle des bassins Néogènes de la région du Cap des Trois Fourches (Rif oriental, Maroc). *Journal of African Earth Sciences (and the Middle East)*, **17**, 233-240.

Azdimousa, A., Jabaloy, A., Asebriy, L., Booth-Rea, G., Gonzalez-Lodeiro, F. & Bourgois, J. (2007). Lithostratigraphy and structure of the Temsamane unit (eastern external Rif, Morocco). *Revista de la Sociedad Geológica de España*, **20**, 187-200.

Azdimousa, A., Poupeau, G., Rezqi, H., Asebriy, L., Bourgois, J. & Aït Brahim, L. (2006). Géodynamique des bordures méridionales de la mer d'Alboran; application de la stratigraphie séquentielle dans le bassin néogène de Boudinar (Rif oriental, Maroc). *Bulletin de l'Institut Scientifique. Rabat*, **28**, 9-18.

Baccour, H., Medhioub, M., Jamoussi, F., Mhiri, T. & Daoud, A. (2008). Mineralogical evaluation and industrial applications of the triassic clay deposits, southern Tunisia. *Materials Characterization*, **59**, 1613-1622.

Baghdad, A., Bouazi, R., Bouftouha, Y., Bouabsa, L. & Fagel, N. (2017). Mineralogical characterization of Neogene clay areas from the Jijel basin for ceramic purposes (N.E. Algeria -Africa). *Applied Clay Science*, **136**, 176-183.

Bain, A.J. (1986). Composition and properties of clays used in various fields of ceramics: Part I. *Ceramic Forum International*, **62**, 536-538.

Beaulieu, J. (1979). *Identification géotechnique des matériaux argileux naturels par la mesure de leur surface spécifique au moyen de bleu de méthylène.* Thèse de troisième cycle. d'Orsay, Orsay, France.

Biscaye, P.E. (1965). Mineralogy and sedimentation of recent deep-sea clay in the Atlantic ocean and adjacent seas and oceans. *Geological Society of America Bulletin*, **76**, 803-832.

Boski, T., Pessoa, J., Pedro, P., Thorez, J., Dias, J.M.A. & Hall, I.R. (1998). Factors governing abundance of hydrolyzable amino acids in the sediments from the N.W. European Continental Margin (47–50°N.). *Progress in Oceanography*, **42**, 145-164.

Brindley G.W. & Nakahira M. (1959). The kaolinite–mullite reaction series: II. Metakolin. *Journal of the American Ceramic Society*, **42** (7), 314–318.

Casagrande, A. (1947). Plasticity chart for the classification of cohesive soils. *Transactions of the American Society of Civil Engineers*, 783–811.

Chalouan, A., Michard, A., Kadiri, K.E., Negro, F., Lamotte, D.F.d., Soto, J.I. & Saddiqi, O. (2008). The Rif Belt. Pp. 203-302. In A. Michard, O. Saddiqi, A. Chalouan, and D. Frizon de Lamotte, Eds. *Continental evolution: The geology of Morocco: Structure, stratigraphy, and tectonics of the Africa-Atlantic-Mediterranean triple junction*, Springer, Berlin.

Cook, H.E., Johnson, P.D., Matti, J.C. & Zemmels, I. (1975). Methods of sample preparation and X-Ray Diffraction data analysis, X-Ray mineralogy laboratory, deep sea drilling project, University of California, Riverside. *Initial Reports of the Deep Sea Drilling Project*, **28**, 999-1007.

Cornée, J.-J., Münch, P., Achalhi, M., Merzeraud, G., Azdimousa, A., Quillévéré, F., Melinte-Dobrinescu, M., Chaix, C., Moussa, A.B., Lofi, J., Séranne, M. & Moissette, P. (2016). The Messinian erosional surface and early Pliocene reflooding in the Alboran sea: New insights from the Boudinar Basin, Morocco. *Sedimentary Geology*, **333**, 115-129.

Cunningham, K.J. & Collins, L.S. (2002). Controls on facies and sequence stratigraphy of an upper Miocene carbonate ramp and platform, Melilla Basin, N.E. Morocco. *Sedimentary Geology*, **146**, 285-304.

Cunningham, K.J., Benson, R.H., Rakic-El Bied, K. & McKenna, L.W. (1997). Eustatic implications of late Miocene depositional sequences in the Melilla Basin, Northeastern Morocco. *Sedimentary Geology*, **107**, 147-165.

De Jong, E. (1999). Comparison of three methods of measuring surface area of soils. *Canadian Journal of Soil Science*, **79**, 345-351.

De Kimpe, C.R., Laverdiere, M.R. & Martel, Y.A. (1979). Surface area and exchange capacity of clay in relation to the mineralogical composition of gleysolic soils. *Revue Canadienne de la Science du Sol*, **59**, 341-347.

Dolinar, B., Mišič, M., Trauner, L. (2007). Correlation between surface area and Atterberg limits of fine-grained soils. *Clays and Clay Minerals*, **55**, 519-523.

Dondi, M. (1999). Clay materials for ceramic tiles from the Sassuolo District (Northern Apennines, Italy). Geology, composition and technological properties. *Applied Clay Science*, **15**, 337-366.

Dondi, M., Raimondo, M. & Zanelli, C. (2014). Clays and bodies for ceramic tiles: Reappraisal and technological classification. *Applied Clay Science*, **96**, 91-109.

El Bakkali, S., Bourdier, J.-L. & Gourgaud, A. (1998a). Caractérisation et stratigraphie de dépôts volcanoclastiques marqueurs dans le Miocène supérieur du bassin de Melilla-bas Kert (Rif Oriental, Maroc). *Comptes Rendus de l'Académie des Sciences - Series IIA - Earth and Planetary Science*, **327**, 93-100.

El Bakkali, S., Gourgaud, A., Bourdier, J.-L., Bellon, H. & Gundogdu, N. (1998b). Post-collision Neogene volcanism of the Eastern Rif (Morocco): Magmatic evolution through time. *Lithos*, **45**, 523-543.

El Boudour El Idrissi, H., Daoudi, L., El Ouahabi, M., Collin, F. & Fagel, N. (2018). The influence of clay composition and lithology on the industrial potential of earthenware. *Construction and Building Materials*, **172**, 650-659.

El Ouahabi, M. (2013). *Valorisation industrielle et artisanale des argiles du Maroc*. PhD thesis in Sciences. Université de Liège.

El Ouahabi, M., Daoudi, L. & Fagel, N. (2014b). Mineralogical and geotechnical characterization of clays from northern Morocco for their potential use in the ceramic industry. *Clay Minerals*, **49**, 35-51.

El Ouahabi, M., Daoudi, L., De Vleeschouwer, F., Bindler, R. & Fagel, N. (2014a). Potentiality of clay raw materials from northern Morocco in ceramic industry: Tetouan and Meknes areas. *Journal of Minerals and Materials Characterization and Engineering*, **2**, 145-159.

El Ouahabi, M., Daoudi, L., Hatert, F. & Fagel, N. (2015). Modified mineral phases during clay ceramic firing. *Clays and Clay Minerals*, **63**, 404-413.

Essafi, M. (1986). *Etude minéralogique et géochimique des bentonites du Rif nord oriental (bassin de Melilla-Nador).* Docteur-Ingénieur. Paris-Sud - Centre d'Orsay-, France.

Fagel, N., Boski, T., Likhoshway, L. & Oberhaensli, H. (2003). Late Quaternary clay mineral record in Central Lake Baikal (Academician

Ridge, Ciberia). *Palaeogeography, Palaeoclimatology, Palaeoecology*, **193**, 159-179.

Fagel, N., Thamó-Bózsó, E. & Heim, B. (2007). Mineralogical signatures of Lake Baikal sediments: Sources of sediment supplies through Late Quaternary. *Sedimentary Geology*, **194**, 37-59.

Ferrari, S. & Gualtieri, A.F. (2006). The use of illitic clays in the production of stoneware tile ceramics. *Applied Clay Science*, **32**, 73-81.

Fiori, C., Fabbri, B., Donati, G. & Venturi, I. (1989). Mineralogical composition of the clay bodies used in the Italian Tile Industry. *Applied Clay Science*, **4**, 461-473.

Frizon de Lamotte, D. & Leikine, M. (1985). Métamorphisme miocène du Rif oriental (Maroc) et individualisation de la nappe gravitaire d'Aknoul. *Revue de géologie dynamique et de géographie physique*, **26**, 29-42.

González, I., Galán, E., & Miras, A. (2006). Fluorine, chlorine and sulphur emissions from the Andalusian ceramic industry (Spain)-Proposal for their reduction and estimation of threshold emission values. *Applied Clay Science*, **32**, 3-4.

González, I., Galán, E., Miras, A., & Aparicio, P. (1998). New uses for brick-making clay from the Bailén area (southern materials Spain). *Clay Minerals*, **33**, 453-465.

Guillemin, M. & Houzay, J.-P. (1982). *Le Néogène post-nappe et le Quaternaire du Rif nord-oriental. Stratigraphie et tectonique des bassins de Melilla, du Kert, de Boudinar, et du piedmont des Kebdana.* Pp. 7. Notes et Mémoires du Service Géologique du Maroc, Rabat.

Harvey, C.C. & Lagaly, G. (2006). Chapter 10.1 conventional applications. Pp. 501-540. In B.K.G.T. Faïza Bergaya, and L. Gerhard, Eds. *Developments in clay science*, Volume 1,Elsevier.

Holtz, R.D. & Kovacs, W.D. (1981). *An introduction to geotechnical engineering*. Pp. 733. Prentice Hall, New Jersey.

Jabaloy-Sánchez, A., Azdimousa, A., Booth-Rea, G., Asebriy, L., Vázquez-Vílchez, M., Martínez-Martínez, J.M. & Gabites, J. (2015). The structure of the Temsamane fold-and-thrust stack (eastern Rif, Morocco): Evolution of a transpressional orogenic wedge. *Tectonophysics*, **663**, 150-176.

Jordán, M. M., Sanfeliu, T., & De la Fuente, C. (2001). Firing transformations of Tertiary clays used in the manufacturing of ceramic tile bodies. *Applied Clay Science*, **20**, 87-95.

Keith, K.S. & Murray, H.H. (2009). Common clays and shale. Pp. 369-371. In J.E. Kogel, N.C. Trivedi, J.M. Barker, and S.T. Krukowski, Eds. *Industrial minerals and rocks. Commodities, markets, and uses*,Society for Mining, Metallurgy, and Exploration, Inc.

Kharbish, S. & Farhat, H.I. (2017). Mineralogy and physico-chemical properties of Wadi Badaa clays (Cairo-Suez district, Egypt): A prospective resource for the ceramic industry. *Arabian Journal of Geosciences*, **10**, 174.

Lisboa, J.V., Rocha, F. & de Oliveira, D.P.S. (2016). Application of multivariate analysis in the assessment of ceramic raw materials. *Clays and Clay Minerals*, **64**, 767-787.

Mahmoudi, S., Bennour, A., Srasra, E. & Zargouni, F. (2017). Characterization, firing behavior and ceramic application of clays from the Gabes region in south Tunisia. *Applied Clay Science*, **135**, 215-225.

Mazzoli, S. & Helman, M. (1994). Neogene patterns of relative plate motion for Africa-Europe: Some implications for recent central Mediterranean tectonics. *Geologische Rundschau*, **83**, 464-468.

Mesrar, L., Akdim, M., Akhrif, I., Lakrim, M., El Aroussi, O., Chaouni, A. & Jabrane, R. (2013). Technological valorization of the Miocene clay in the region of Fez (Morocco): Characterisation and exploitation possibilities. *Present Environment and Sustainable Development*, **7**, 310-317.

Mesrar, L., Lakrim, M., Akdim, M., Benamar, A., Es–Sbai, N. & Jabrane, R. (2017). Preparation and characterization of Miocene clay powders in the region of Taza (Morocco) after doping with metal oxides $Al_2O_3$. *Proceedings of the XII Maghreb Days of Material Sciences-Materials Science and Engineering*, Fez, Morocco, 2017, IOP science, Pp. 1-9.

Michard, A., Chalouan, A., Feinberg, H., Goffé, B. & Montigny, R. (2002). How does the Alpine Belt end between Spain and Morocco ? *Bulletin de la Société Géologique de France*, **173**, 3-15.

Milheiro, F.A.C., Freire, M.N., Silva, A.G.P. & Holanda, J.N.F. (2005). Densification behaviour of a red firing Brazilian kaolinitic clay. *Ceramics International*, **31**, 757-763.

Milošević, M. & Logar, M. (2017). Properties and characterization of a clay raw material from Miličinica (Serbia) for use in the ceramic industry. *Clay Minerals*, **52**, 329–340.

Moore, D.M. & Reynold, R.C. (1997). *X-Ray Diffraction and the identification and analysis of clay minerals*. Second Edition. Pp. 378. Oxford University Press, Inc.

Mukherjee, S. (2013). *The science of clays. Applications in industry, engineering and environment*. First Edition. Pp. 335. Capital Publishing Company.

Münch, P., Cornée, J.J., Féraud, G., Martin, J.P.S., Ferrandini, M., Garcia, F., Conesa, G., Roger, S. & Moullade, M. (2006). Precise $^{40}Ar/^{39}Ar$ dating of volcanic tuffs within the upper Messinian sequences in the Melilla carbonate complex (N.E. Morocco): Implications for the Messinian Salinity Crisis. *International Journal of Earth Sciences*, **95**, 491-503.

Murray, H.H. (1994). Common clays. Pp. 247–248. In D.D. Carr, Ed. *Industrial minerals and rocks*, Society for Mining, Metallurgy and Exploration, Littleton, CO.

Murray, H.H. (2007). *Applied clay mineralogy: Occurrences, processing and application of kaolins, bentonites, palygorskite-sepiolite, and common clays*. Pp. 180. Elsevier.

Nasri, H., Elhammouti, K., Azdimousa, A., Achalhi, M. & Bengamra, S. (2016). Calcimetric and sedimentometric characterization of clay deposits in the Neogene Boudinar basin (north eastern Rif, Morocco): Implication on the eustatic and hydrodynamic evolution of the basin and economic interest. *Journal of Materials and Environmental Science*, **7**, 859-870.

Negro, F., de Sigoyer, J., Goffé, B., Saddiqi, O. & Villa, I.M. (2008). Tectonic evolution of the Betic–Rif arc: New constraints from $^{40}Ar/^{39}Ar$ dating

on white micas in the Temsamane units (External Rif, northern Morocco). *Lithos*, **106**, 93-109.

Ngun, B.K., Mohamad, H., Sulaiman, S.K., Okada, K. & Ahmad, Z.A. (2011). Some ceramic properties of clays from central Cambodia. *Applied Clay Science*, **53**, 33-41.

Nkalih Mefire, A., Yongue Fouateu, R., Njoya, A., Mache, J.R., Pilate, P., Hatert, F. & Fagel, N. (2018). Mineralogy and geochemical features of Foumban clay deposits (West Cameroon): genesis and Potential applications. *Clay Minerals*, **53**, 431-445.

Olchawa, A., Gorączko, A.(2012). The relationship between the liquid limit of clayey soils, external specific surface area and the composition of exchangeable cations. *Journal of Water and Land Development*, **17**, 83-88.

Petersen, L.W., Moldrup, P., Jacobsen, O.H. & Rolston, D.E. (1996). Relations between specific surface area and soil physical and chemical properties. *Soil Science*, **161**, 9-21.

Petrick, K., Diedel, R., Peuker, M., Dieterle, M., Kuch, P., Kaden, R., Krolla-Sidenstein, P., Schuhmann, R. & Emmerich, K. (2011). Character and amount of I-S mixed-layer minerals and physical-chemical parameters of two ceramic clays from Westerwald, Germany: Implications for processing properties. *Clays and Clay Minerals*, **59**, 58-74.

Polidori, E. (2007). Relatioship between the Atterberg limits and clay content. *Soils and Foundations*, **47**, 887-896.

Reeves, G.M., Sims, I. & Cripps, J. (2006). *Clay materials used in construction*. Pp. 1-447. Geological Society, London.

Rosenbaum, G., Lister, G.S. & Duboz, C. (2002). Relative motions of Africa, Iberia and Europe during Alpine orogeny. *Tectonophysics*, **359**, 117–129.

Shepard, F.P. (1954). Nomenclature based on sand–silt–clay ratios. *Journal of Sedimentary Petrology*, **24**, 151-158.

Shvarzman, A., Kovler, K.G., Grader, G.S. & Shter, E. (2003). The effect of dehydroxylation/amorphization degree on pozzolanic activity of kaolinite. *Cement and Concrete Research*, **33**, 405-416.

Strazzera, B., Dondi, M. & Marsigli, M. (1997). Composition and ceramic properties of Tertiary clays from southern Sardinia (Italy). *Applied Clay Science*, **12**, 247-266.

Tiller, K.G. & Smith, L.H. (1990). Limitations of EGME retention to estimate the surface area of soils. *Australian Journal of Soil Research*, **28**, 1-26.

Trindade, M.J., Dias, M.I., Coroado, J. & Rocha, F. (2009). Mineralogical transformations of calcareous rich clays with firing: A comparative study between calcite and dolomite rich clays from Algarve, Portugal. *Applied Clay Science*, **42**, 345-355.

Trindade, M.J., Dias, M.I., Coroado, J.o. & Rocha, F. (2010). Firing tests on clay-rich raw materials from the Algarve basin (southern Portugal): Study of mineral transformations with temperature. *Clays and Clay Minerals*, **58**, 188-204.

Van Assen, E., Kuiper, K.F., Barhoun, N., Krijgsman, W. & Sierro, F.J. (2006). Messinian astrochronology of the Melilla basin: Stepwise restriction of the Mediterranean–Atlantic connection through Morocco. *Palaeogeography, Palaeoclimatology, Palaeoecology*, **238**, 15-31.

Wattanasiriwech, D., Srijan, K. & Wattanasiriwech, S. (2009). Vitrification of illitic clay from Malaysia. *Applied Clay Science*, **43**, 57-62.

Wentworth, C.K. (1922). A scale of grade and class terms for clastic sediments. *The Journal of Geology*, **30**, 377-392.

Winkler, H.G.F. (1954). Bedeutung der korngrössenverteilung und des mineralbestandes von tonen für die herstellung grobkeramischer erzeugnisse. *Berichte der Deutschen Keramischen Gesellschaft*, **31**, 337-343.

**FIGURES CAPTION**

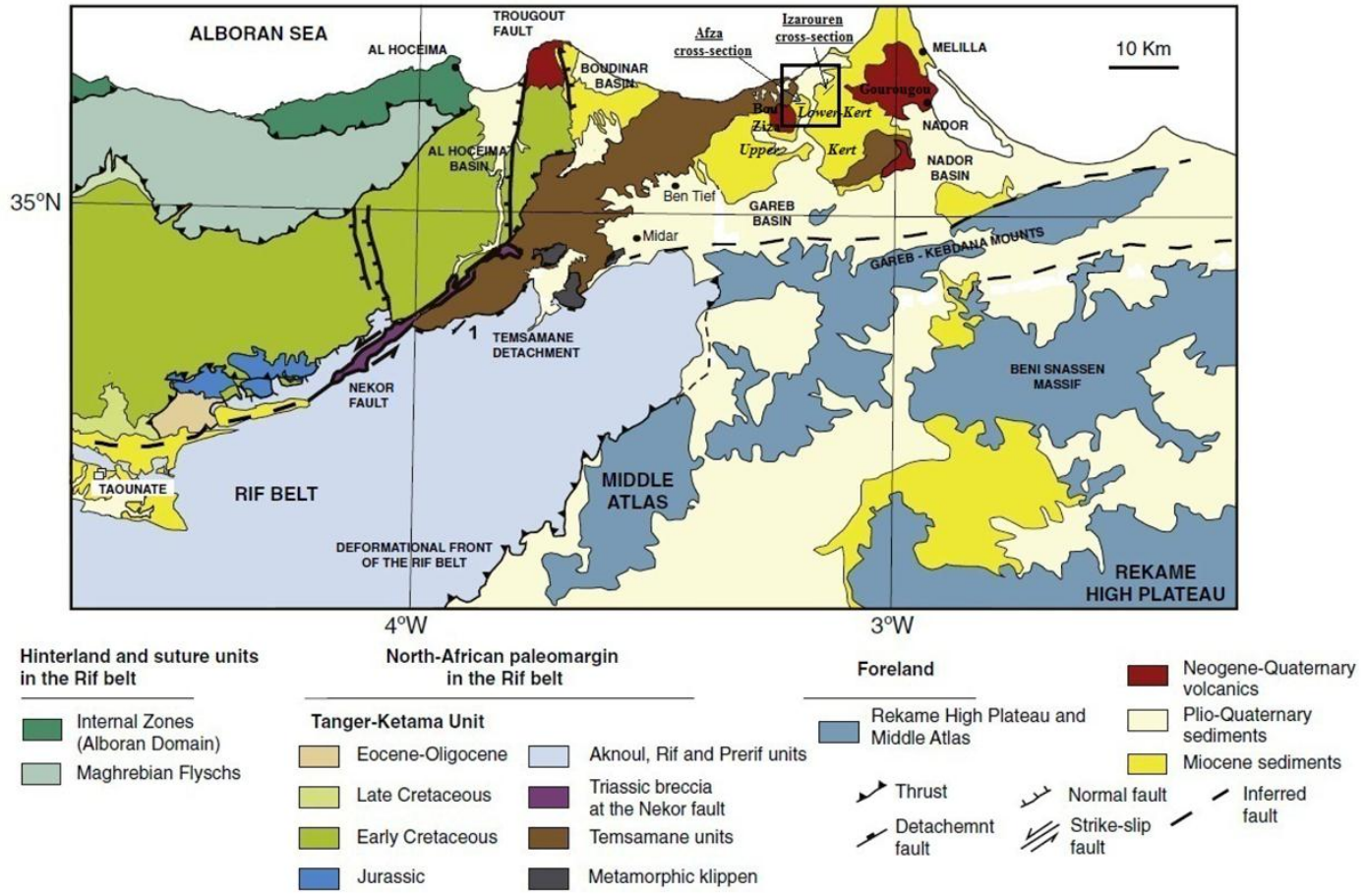


FIG. 1. Study area location in the geological map of the north-eastern Rif (Morocco) (Jabaloy-Sánchez *et al.*, 2015), modified.



DOI: 10.1180/clm.2019.50

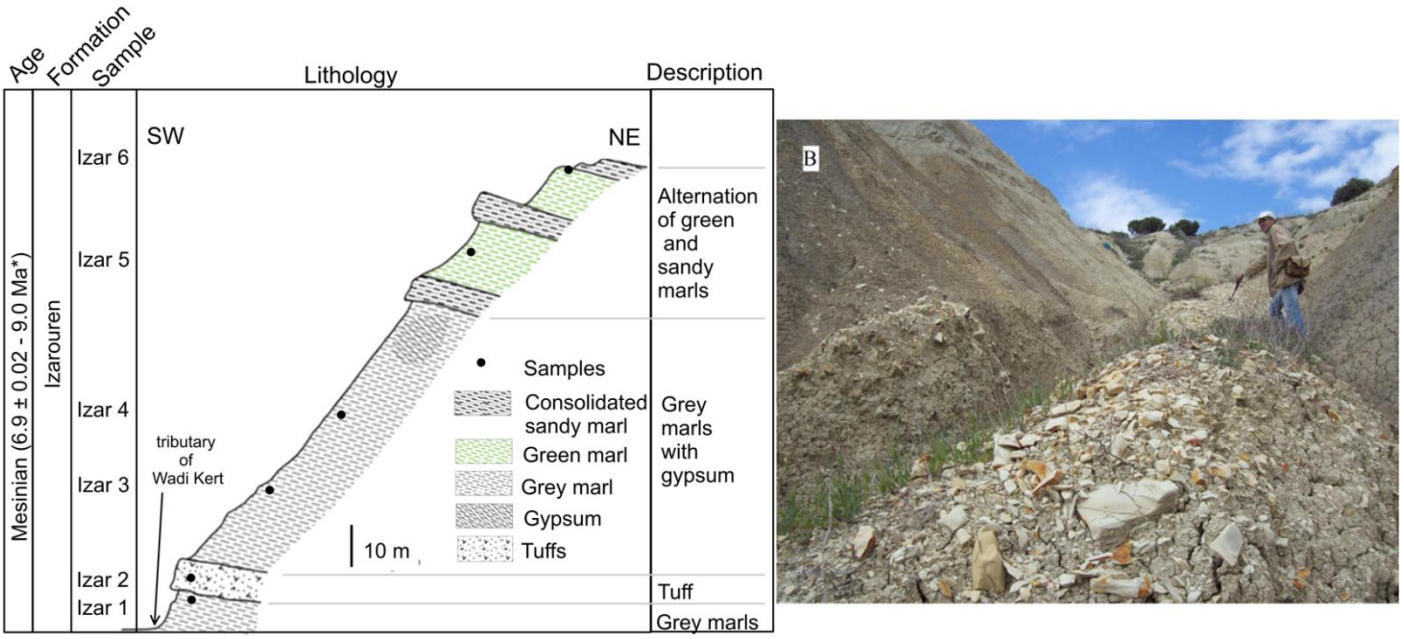


FIG. 2. Lithological section of the Izaroren profile and corresponding photograph.

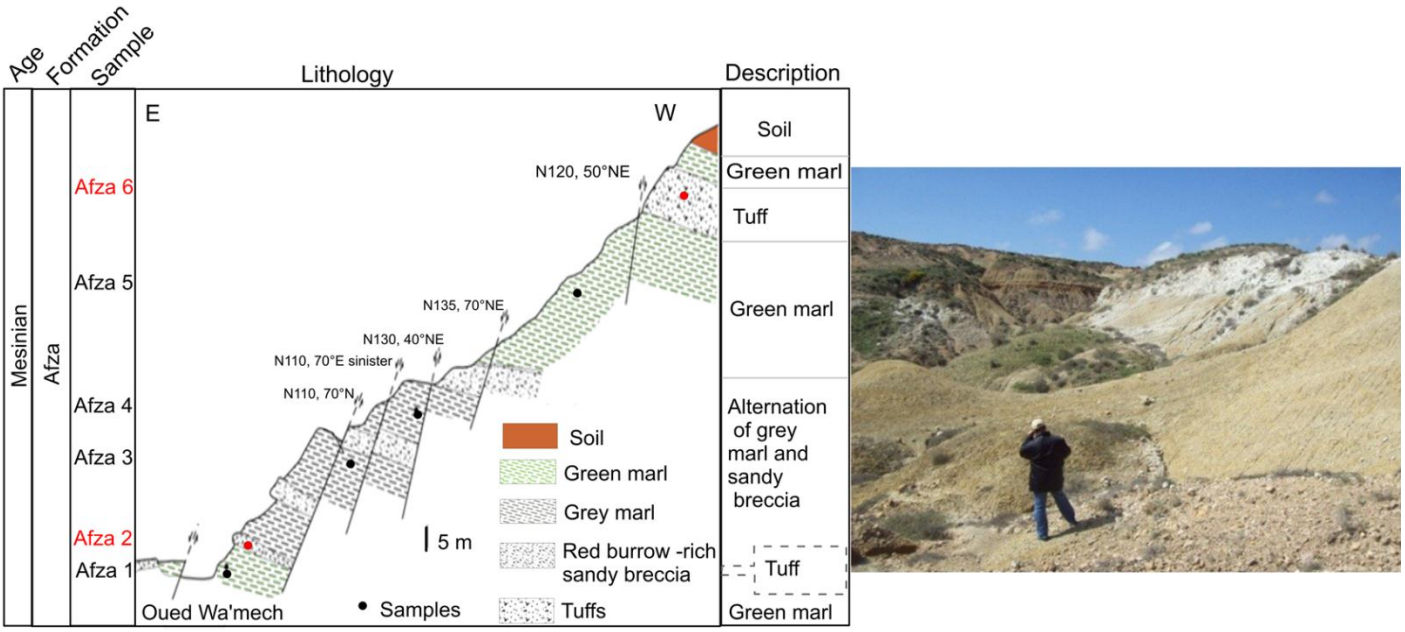


FIG. 3. Lithological description of the Afza profile and photograph illustrating the studied facies.

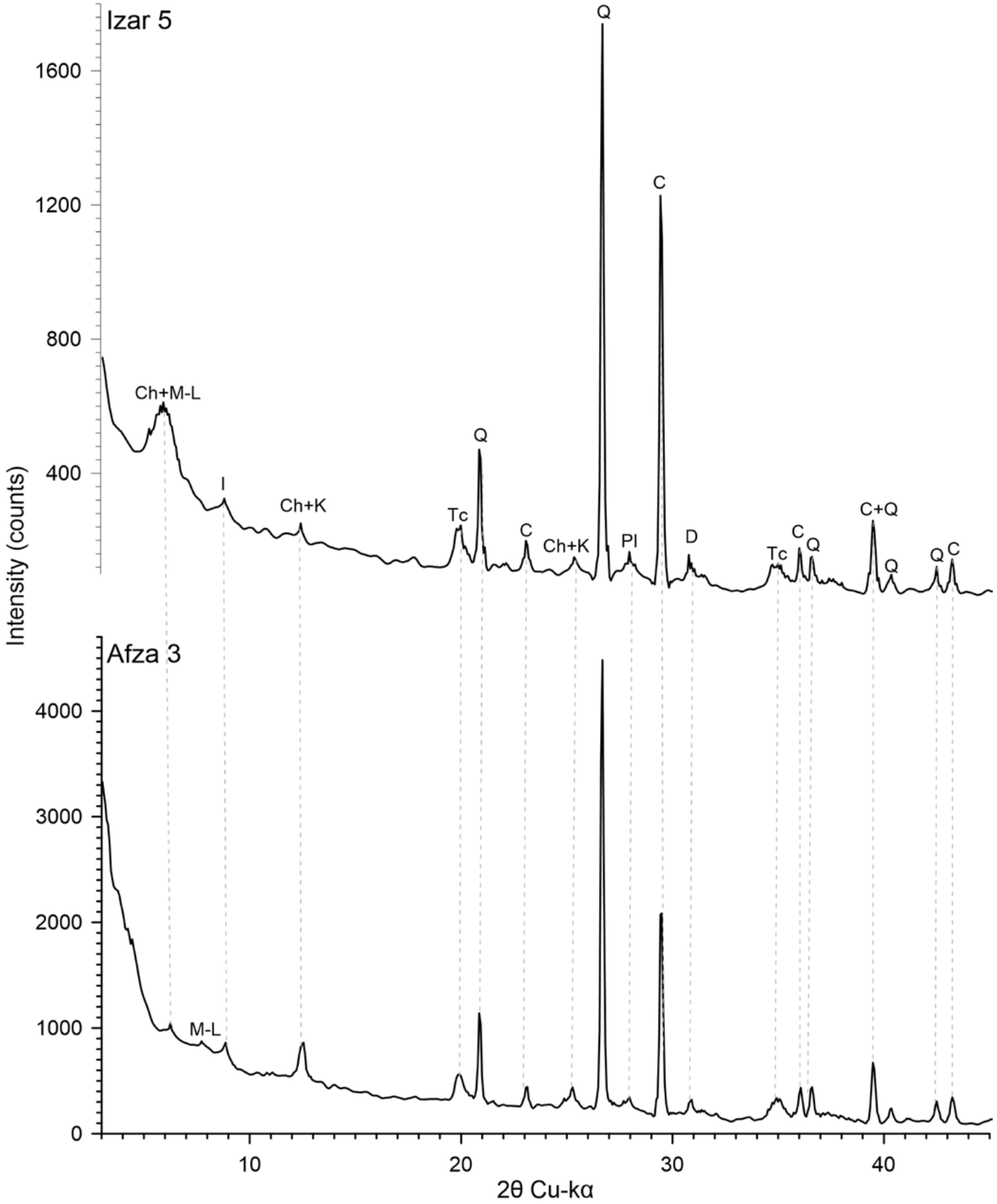


FIG. 4. XRD pattern of unoriented powders of Izaroren 5 and Afza 3 samples: M-L-Mixed-layer, Ch-Chlorite, I-Illite, K-Kaolinite, Tc-Total caly, Q-Quartz, C-Calcite, Pl-Plagioclase, and D-Dolomite.

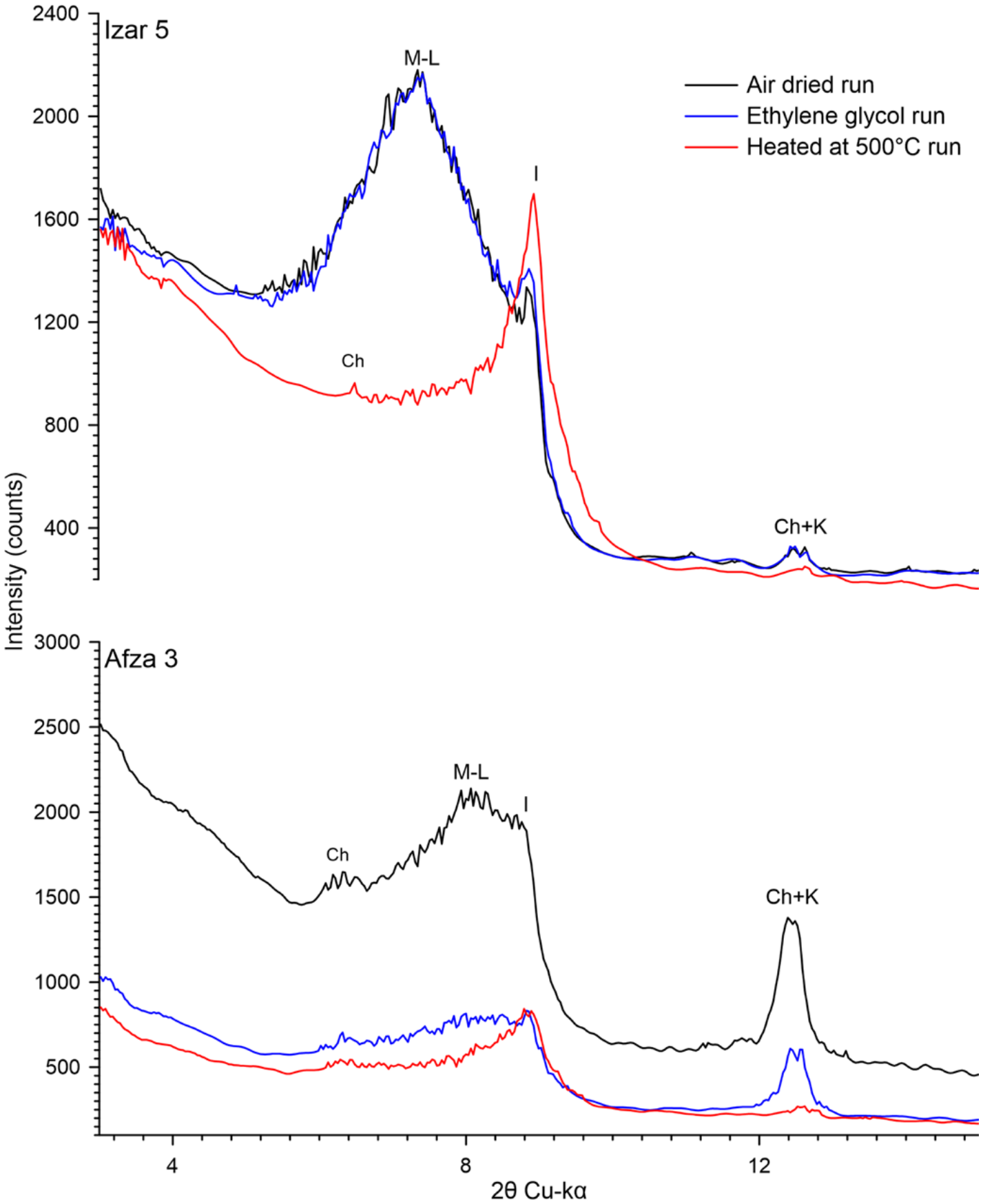


FIG. 5. XRD pattern of oriented Izaroren 5 and Afza 3 samples: M-L-Mixed-layer, Ch-Chlorite, I-Illite, K-Kaolinite.

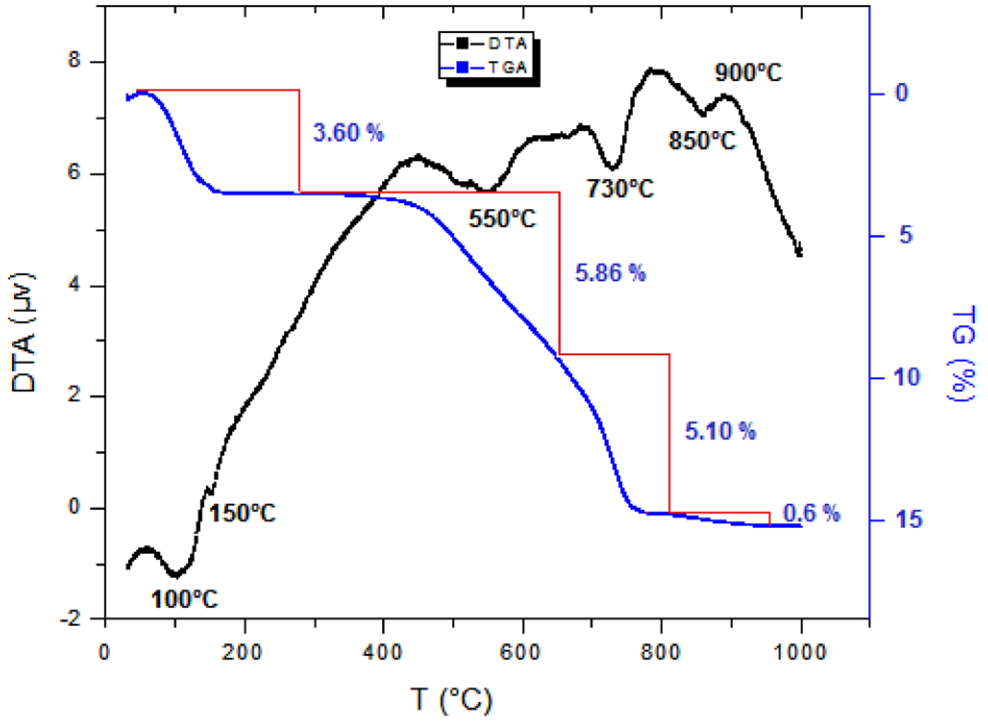


FIG. 6. DTA/TG curves of Izaroren 4 sample.

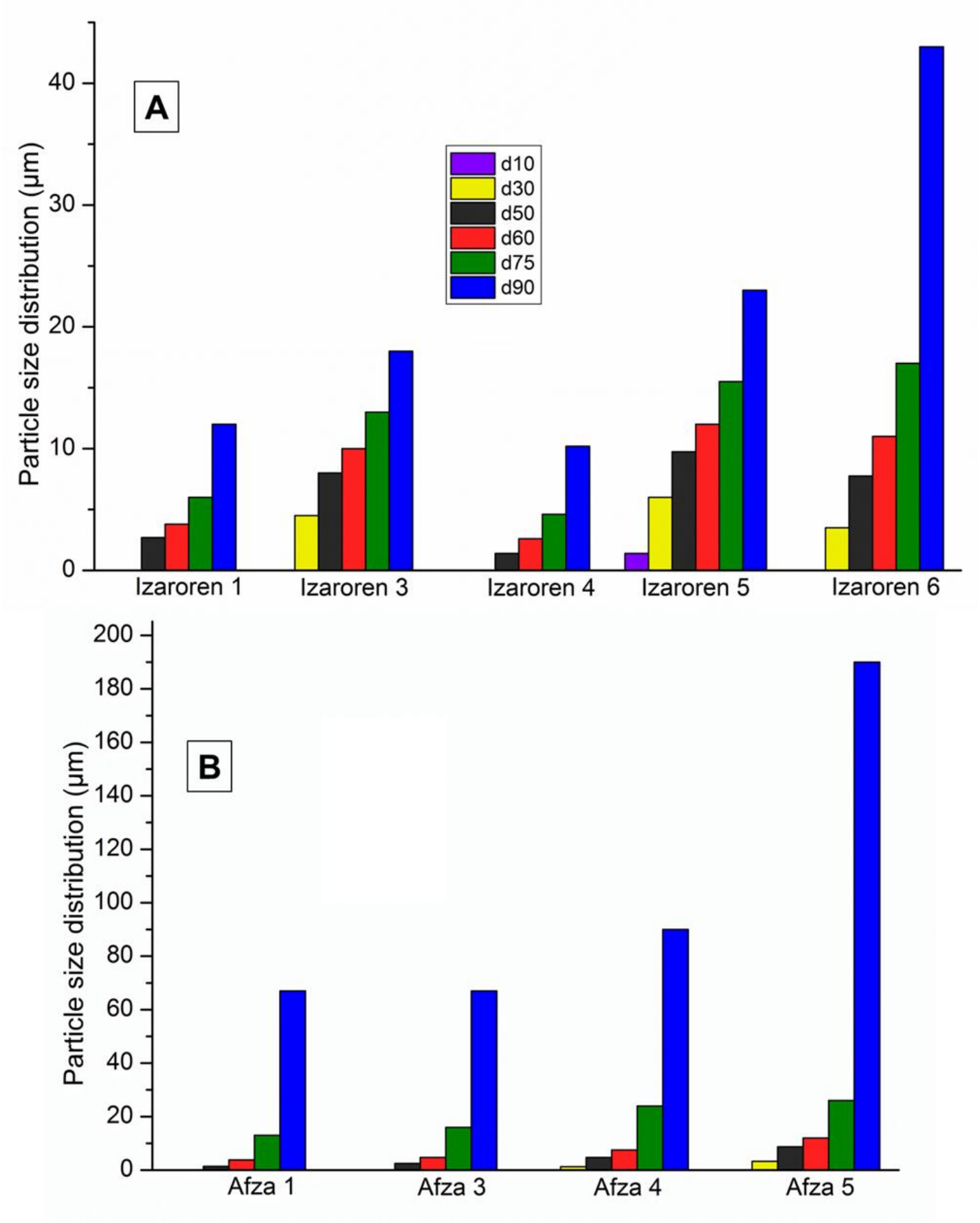


FIG. 7. Particle size distribution along (A) Izaroren and (B) Afza profiles based on d10, d30, d50, d60, d75 and d90 parameters.

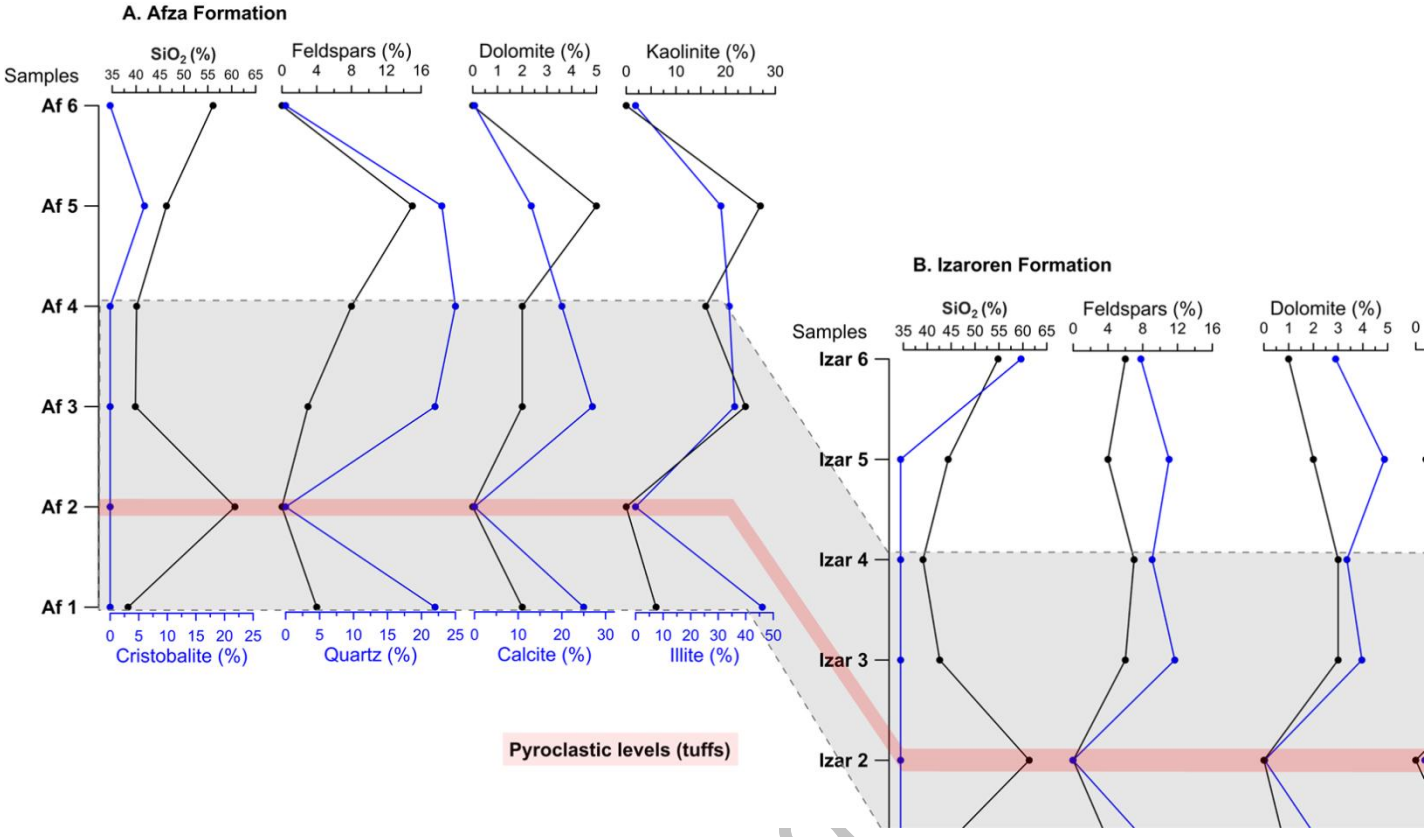


FIG. 8. Correlation between Izaroren and Afza profiles based on pyroclastic layers and mineralogical composition.

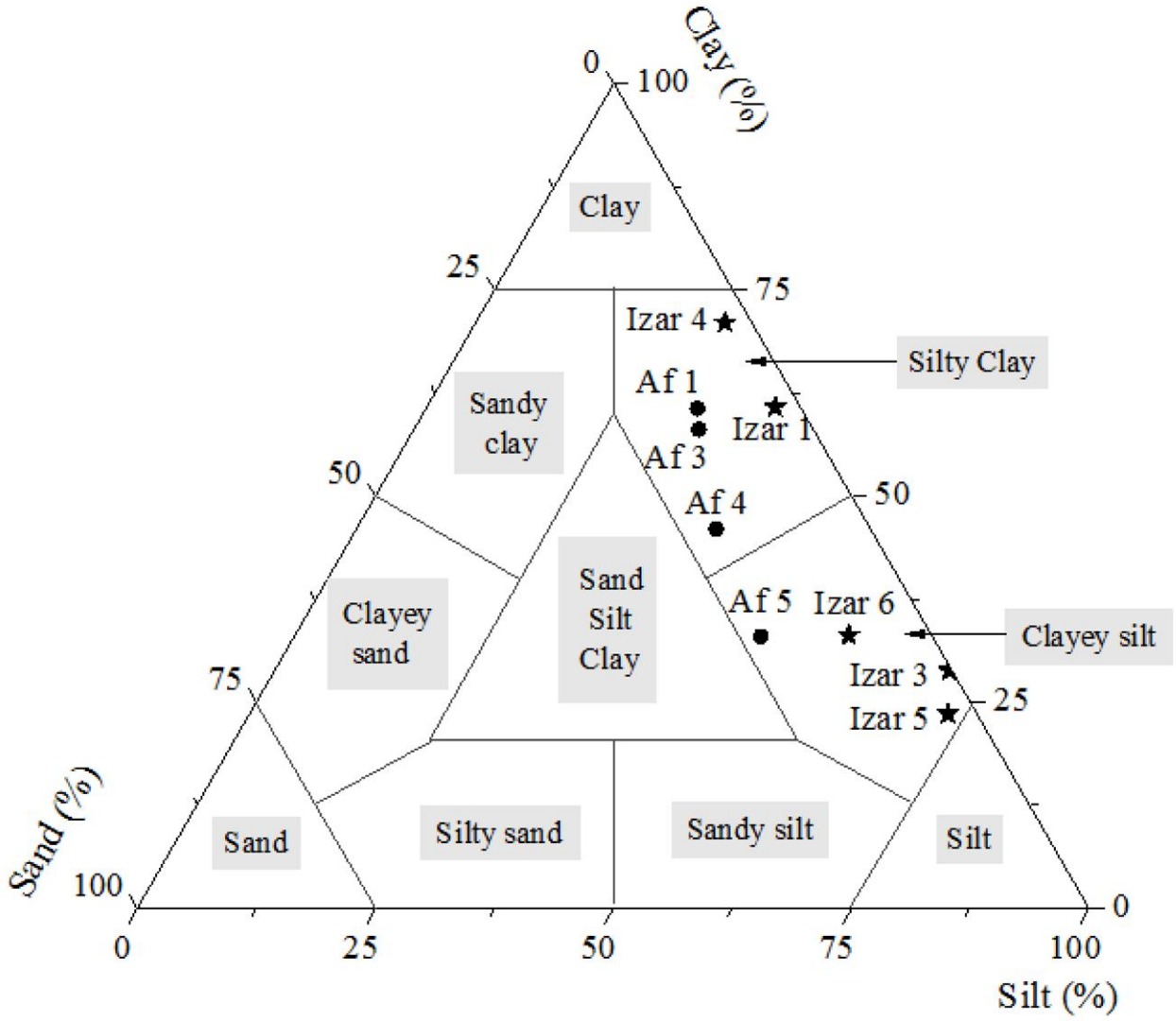


FIG. 9. Plot of grain-size results of studied samples in Shepard ternary diagram (Shepard, 1954).

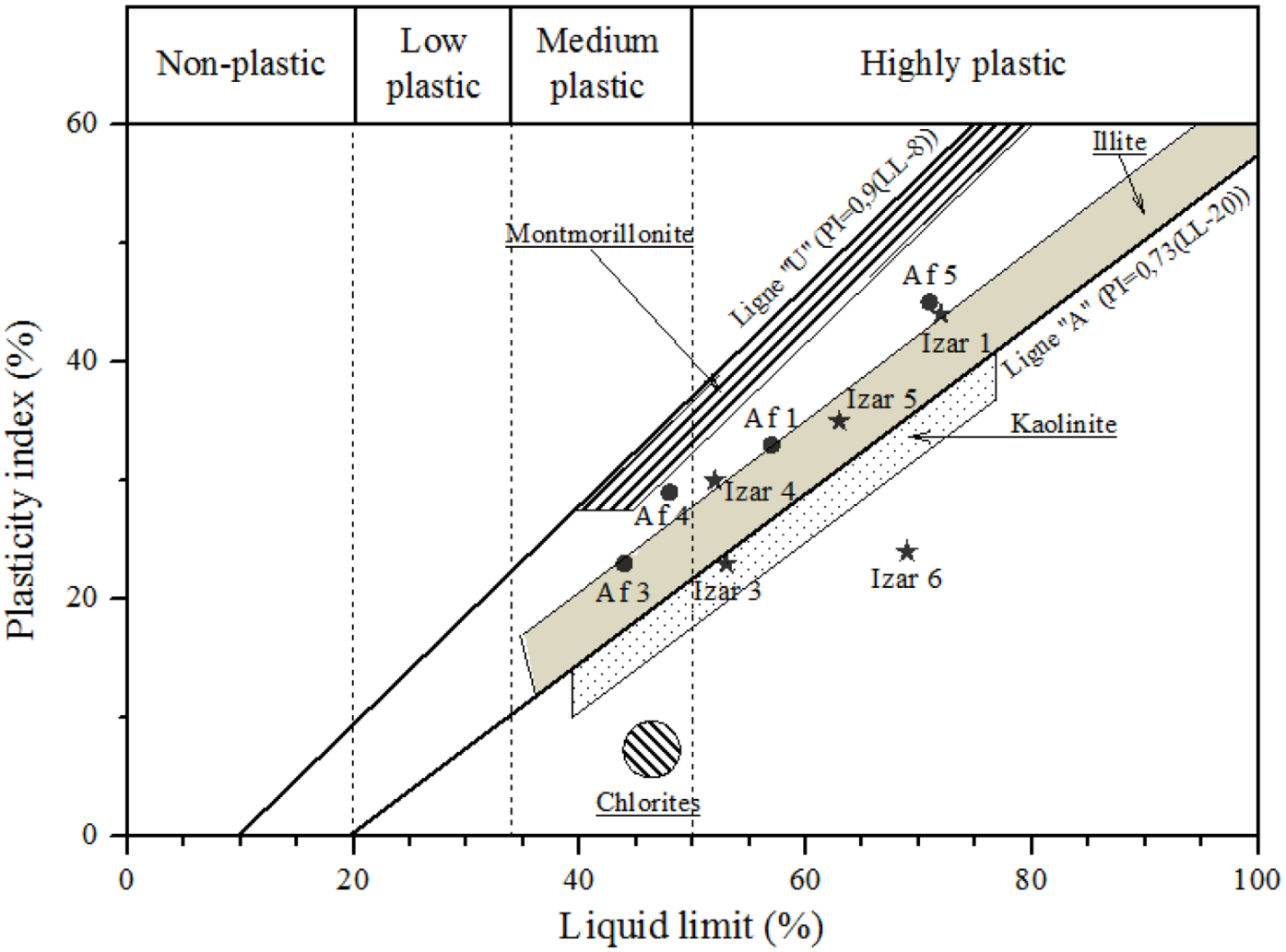


FIG. 10. Plot of studied samples in plasticity chart (Casagrande, 1947; Holtz & Kovacs, 1981).

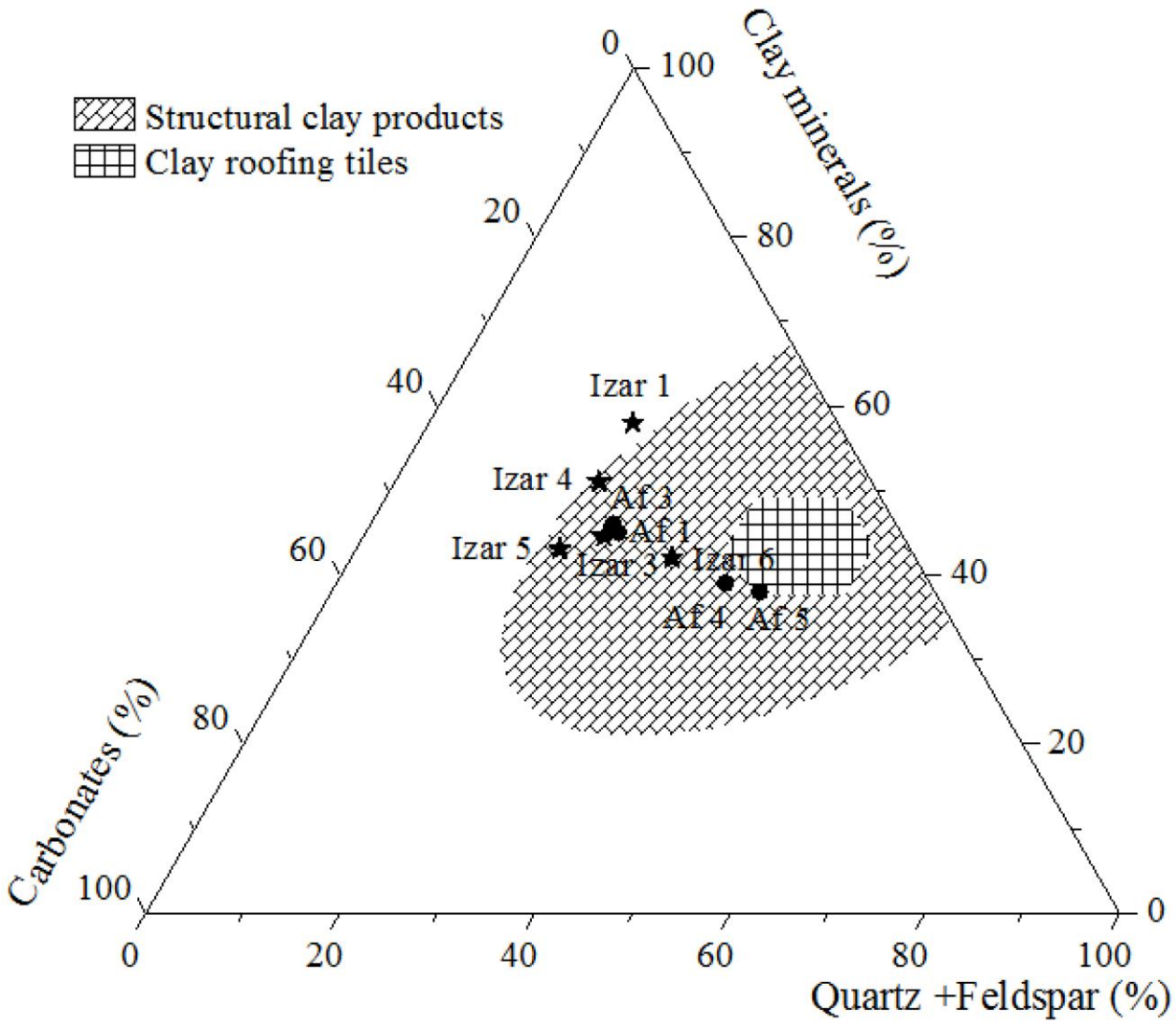


FIG. 11. Classification of studied samples based on Strazzera ternary diagram (Strazzera *et al.*, 1997).

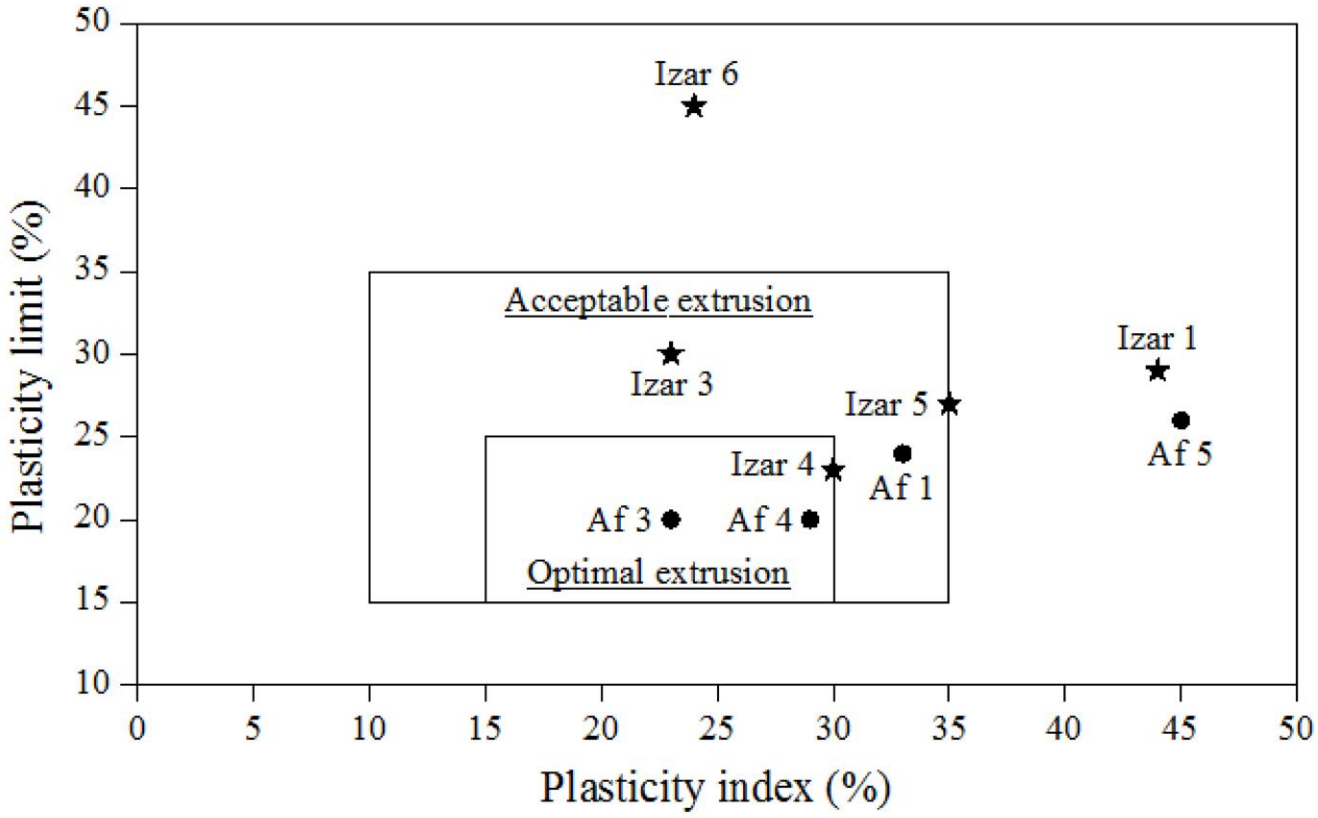


Fig. 12. Bain diagram showing the potential molding of the studied samples (Bain, 1986).

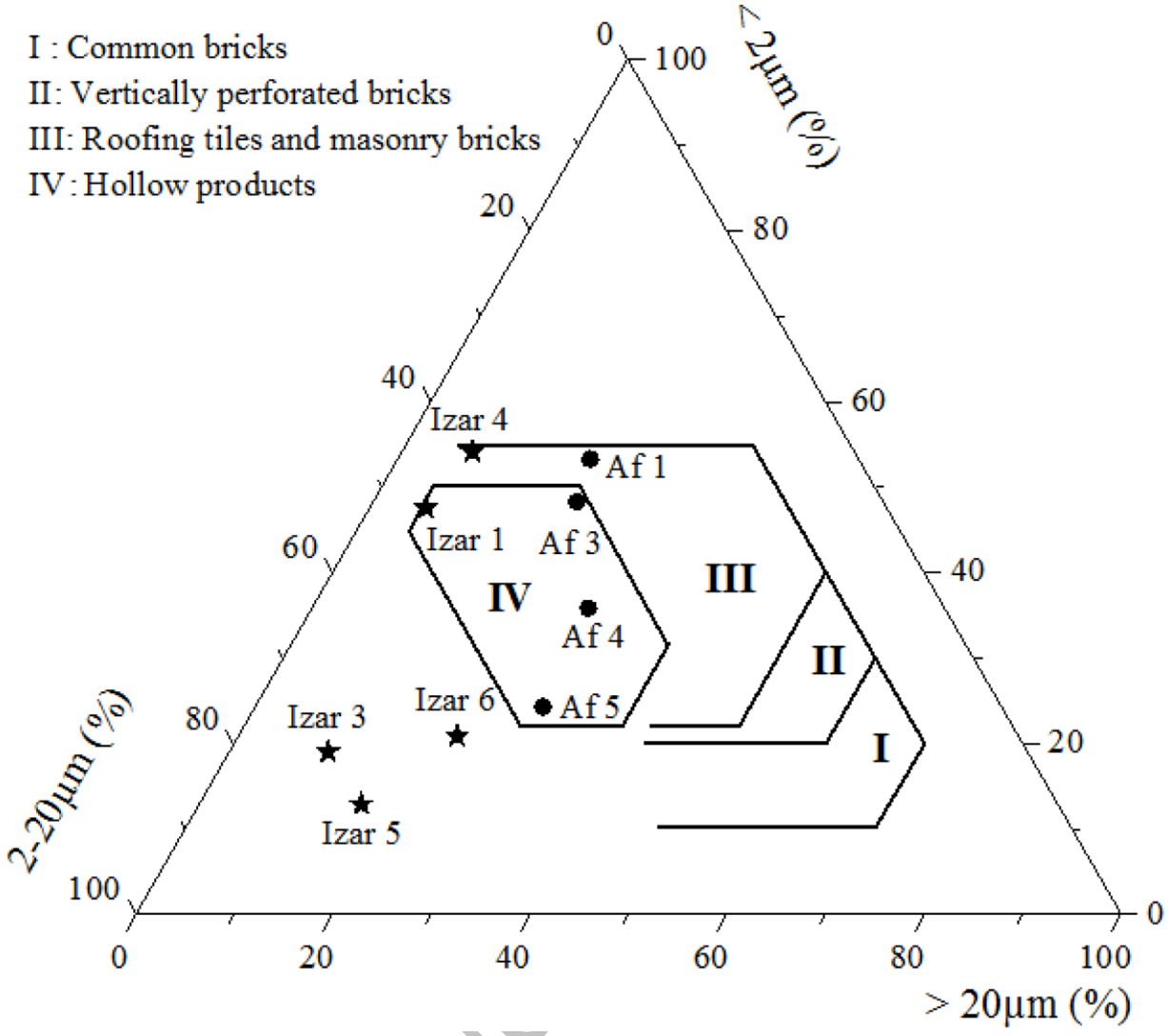


FIG. 13. Plot of studied samples in Winkler ternary diagram (Winkler, 1954).

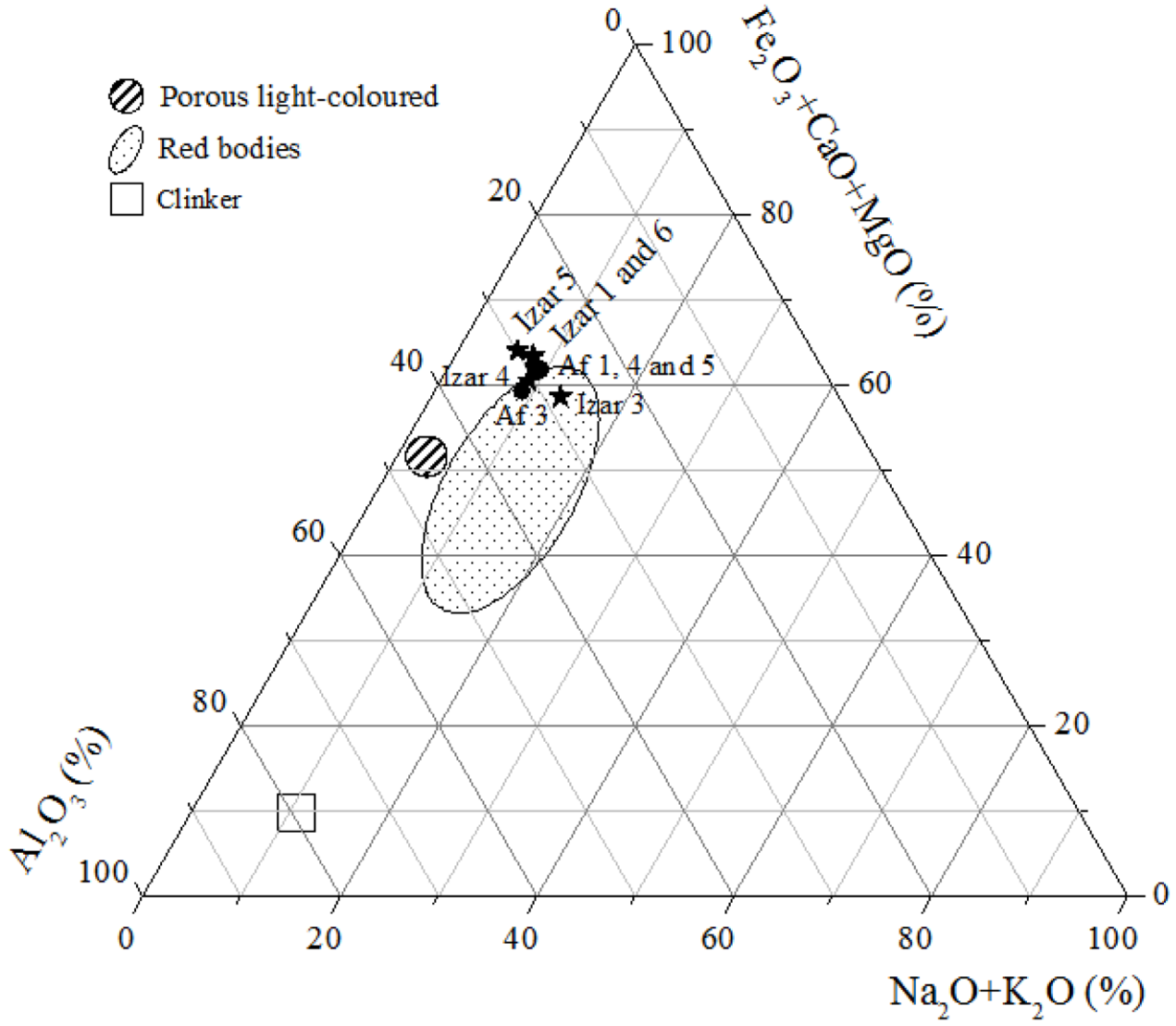


FIG. 14. Plot of studied samples in ($Al_2O_3$)-($Fe_2O_3$+CaO+MgO)-($Na_2O$+$K_2O$) ternary diagram (Fiori *et al.*, 1989).

TABLE 1. Bulk and clay mineralogy of studied samples. Qz: quartz. K-F: Potassium feldspar. Pl: plagioclase. Cc: calcite. Do: dolomite. Sid: siderite. Cris: Cristobalite. Rhod: Rhodochrosite. Amp: Amphibole. I: illite. K: kaolinite. Ch: chlorite.

| Profiles | Bulk mineralogy (wt.%) | | | | | | | | | | | Clay mineralogy (< 2 µm) (wt.%) | | | |
|---|---|---|---|---|---|---|---|---|---|---|---|---|---|---|---|
| | Minerals | Total clay | Qz | K-F | Pl | Cc | Do | Sid | Cris | Rhod | Mica | Amp | I | K | Ch | Mixed-layers |
| Izaroren | Izar 1 | 58 | 16 | 3 | 2 | 18 | 1 | 1 | 0 | 1 | - | - | 28 | 9 | 29 | 34 |
| | Izar2 (tuff) | 50 | 7 | 9 | 16 | 0 | 0 | 0 | 0 | 0 | 10 | 8 | - | - | - | - |
| | Izar 3 | 45 | 18 | 0 | 6 | 26 | 3 | 0 | 0 | 2 | - | - | 32 | 19 | 14 | 35 |
| | Izar 4 | 51 | 14 | 3 | 4 | 22 | 3 | 1 | 0 | 2 | - | - | 35 | 21 | 11 | 33 |
| | Izar 5 | 43 | 17 | 0 | 4 | 32 | 2 | 0 | 0 | 2 | - | - | 29 | 2 | 21 | 48 |
| | Izar 6 | 39 | 12 | 3 | 3 | 19 | 1 | 0 | 22 | 1 | - | - | 40 | 22 | 0 | 38 |
| Afza | Af 1 | 45 | 22 | 0 | 4 | 25 | 2 | 0 | 0 | 2 | - | - | 46 | 6 | 16 | 32 |
| | Af 2 (tuff) | 34 | 4 | 0 | 33 | 6 | 0 | 0 | 7 | 10 | 6 | - | - | - | - | - |
| | Af 3 | 46 | 22 | 0 | 3 | 27 | 2 | 0 | 0 | 0 | - | - | 36 | 24 | 14 | 26 |
| | Af 4 | 42 | 25 | 4 | 4 | 20 | 2 | 1 | 0 | 2 | - | - | 34 | 16 | 20 | 30 |
| | Af 5 | 38 | 23 | 0 | 15 | 13 | 5 | 0 | 6 | 0 | - | - | 31 | 27 | 0 | 42 |
| | Af 6 (tuff) | 8 | 1 | 0 | 79 | 5 | 0 | 0 | 0 | 2 | 5 | 0 | - | - | - | - |



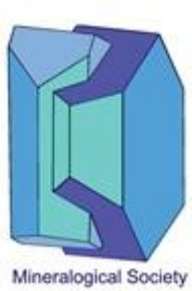


This is a 'preproof' accepted article for Clay Minerals. This version may be subject to change during the production process.

DOI: 10.1180/clm.2019.50

TABLE 2. Geochemical composition in wt.% (* in ppm) and Loss-On Ignition percentage of the studied samples .

| Profiles | Samples | $SiO_2$ | $Al_2O_3$ | $TiO_2$ | $Fe_2O_3$ | CaO | MgO | $K_2O$ | $Na_2O$ | $SO_3$ | S* | $MnO_2$ | $P_2O5$ | L.O.I | Total |
|---|---|---|---|---|---|---|---|---|---|---|---|---|---|---|---|
| Izaroren | Izar 1 | 40.78 | 11.52 | 0.64 | 15.95 | 7.92 | 2.66 | 1.57 | 1.76 | 1.10 | 4406 | 0.46 | 0.19 | 15.32 | 99.9 |
| | Izar 2 (tuff) | 61.33 | 12.33 | 0.14 | 9.67 | 0.92 | 1.03 | 2.76 | 4.73 | 0.46 | 1842 | 0.00 | 0.11 | 6.07 | 99.6 |
| | Izar 3 | 42.60 | 12.02 | 0.65 | 15.13 | 8.12 | 2.98 | 1.58 | 4.28 | 0.59 | 2363 | 0.46 | 0.20 | 11.37 | 100 |
| | Izar 4 | 39.11 | 12.51 | 0.61 | 14.73 | 8.66 | 2.51 | 1.54 | 2.27 | 0.63 | 2523 | 0.40 | 0.19 | 16.85 | 100 |
| | Izar 5 | 44.39 | 10.99 | 0.52 | 13.09 | 9.20 | 2.29 | 1.28 | 1.04 | 0.50 | 2003 | 0.38 | 0.20 | 16.12 | 100 |
| | Izar 6 | 54.82 | 8.48 | 0.37 | 9.13 | 8.70 | 1.75 | 1.09 | 1.34 | 0.30 | 1202 | 0.29 | 0.15 | 13.58 | 100 |
| Afza | Af 1 | 38.32 | 12.13 | 0.57 | 16.60 | 8.38 | 2.36 | 1.45 | 2.71 | 0.46 | 1842 | 0.45 | 0.18 | 16.39 | 100 |
| | Af 2 (tuff) | 60.67 | 13.70 | 0.43 | 3.16 | 2.79 | 2.51 | 1.00 | 6.74 | 0.28 | 1121 | 0.08 | 0.10 | 8.55 | 100 |
| | Af 3 | 39.85 | 13.11 | 0.65 | 14.27 | 8.94 | 2.33 | 1.52 | 2.28 | 0.67 | 2683 | 0.49 | 0.19 | 15.54 | 99.9 |
| | Af 4 | 40.11 | 11.82 | 0.65 | 15.62 | 8.12 | 2.30 | 1.67 | 2.17 | 0.82 | 3284 | 0.51 | 0.19 | 14.67 | 98.6 |
| | Af 5 | 46.37 | 10.80 | 0.56 | 15.46 | 6.57 | 2.27 | 1.41 | 2.32 | 0.49 | 1962 | 0.47 | 0.16 | 13.13 | 100 |
| | Af 6 (tuff) | 56.08 | 11.61 | 0.44 | 4.83 | 5.76 | 1.91 | 1.05 | 6.42 | 0.29 | 1161 | 0.12 | 0.08 | 11.40 | 100 |

TABLE 3. Carbonate content, grain-size, Atterberg limits, and Specific Surface Area results of the studied marly samples.

| Profiles | Izaroren | | | | | Afza | | | |
|---|---|---|---|---|---|---|---|---|---|
| Samples | Izar 1 | Izar 3 | Izar 4 | Izar 5 | Izar 6 | Af 1 | Af 3 | Af 4 | Af 5 |
| Total $CaCO_3$ (wt.%) | 19 | 17 | 20 | 20 | 19 | 17 | 20 | 18 | 13 |
| Particle size distribution (wt.%) | | | | | | | | | |
| < 2 µm | 48 | 19 | 54 | 13 | 21 | 53 | 48 | 36 | 24 |
| 2-20 µm | 47 | 71 | 39 | 71 | 57 | 27 | 31 | 36 | 46 |
| > 20 µm | 6 | 10 | 7 | 16 | 22 | 20 | 21 | 28 | 29 |
| Clay (< 4 µm) | 61 | 29 | 71 | 23 | 33 | 61 | 58 | 46 | 33 |
| Silt (4-63 µm) | 37 | 71 | 26 | 75 | 58 | 29 | 30 | 38 | 49 |
| Sand (> 63 µm) | 3 | 0 | 3 | 2 | 9 | 11 | 12 | 16 | 18 |
| Atterberg limits (%) | | | | | | | | | |
| LL | 72 | 53 | 52 | 63 | 69 | 57 | 44 | 48 | 71 |
| PL | 29 | 30 | 23 | 27 | 45 | 24 | 20 | 20 | 26 |
| PI | 44 | 23 | 30 | 35 | 24 | 33 | 23 | 29 | 45 |
| Specific Surface Area ($m^2/g$) | 89.1 | 73.9 | 89.5 | 70.0 | 26.3 | 88.3 | 107.7 | 90.8 | 125.6 |